UNIVERSITY OF PARDUBICE

FACULTY OF CHEMICAL TECHNOLOGY

Department of General and Inorganic Chemistry

Vít Kremláček

The Reactivity of Latent Heterocyclic Dienes Containing Phosphorus and Arsenic

Theses of the Doctoral Dissertation

Pardubice 2021

Study program: **Inorganic Chemistry**

Study field: **Inorganic Chemistry**

Author: **Vít Kremláček**

Supervisor: **doc. Ing. Libor Dostál, Ph.D.**

Year of the defence: 2021

References

KREMLÁČEK, Vít. *The Reactivity of Latent Heterocyclic Dienes Containing Phosphorus and Arsenic*. Pardubice, 2018. 128 pages. Dissertation thesis (PhD.). University of Pardubice, Faculty of chemical Technology, Department of General and Inorganic Chemistry

Abstract

This thesis is focused mainly on the study of the reactivity of C,N and N,C,N chelated fosfinidenes and arsinidenes. Prepared compounds were subsequently also characterized. The theoretical part is drafted as a literary search dealing with the preparation and reactivity of pnictinidenes and several heteropnictoles. The discussion is dedicated in the first part toward the unique ambiguous behaviour of the N,C,N chelated phosphinidenes and arsinidenes, which allows them to act as either four-electron donors, or heterodienes in hetero-Diels-Alder [4+2] cycloaddition. The following part demonstrates this presupposition on the reativity of a C,N chelated fosfinidene. The discussion then focuses on the reactivity of C,N and N,C,N chelated arsinidenes toward electron-poor alkynes, which is followed by a comprehensive study regarding the reactivity of fosfinidenes and arsinidenes toward *N*-substituted maleimides, while also discussing this reactivity in the comparison with structurally related stibinidenes and bismuthinidenes. The final part of the discussion concerns itself with the preparation and reactivity of an arsinidene chelated by an unsymmetrical N,C,N ligand containing one amine and one imine donor group. Prepared compounds are characterized by multinuclear NMR spectroscopy, X-ray diffraction crystallography, infrared and Raman spectroscopy, mass spectrometry, elemental analysis and their melting point was estimated.

Keywords

Phosphorus, arsenic, chelating ligand, pnictiniden, 2,1-benzazapnictol, hetero-Diels-Alder cycloaddition, cooridnation compounds

Abstrakt

Tato práce se věnuje převážně studiu reaktivity C,N a N,C,N chelatovaných fosfinidenů a arsinidenů. Připravené produkty jsou následně také charakterizovány. Teoretická část je pojata jako rešerše přípravy a reaktivity pniktinidenů a některých heteropniktolů. Diskuze je věnována nejprve unikátnímu nejednoznačnému chování N,C,N chelatovaných fosfinidenů a arsinidenů, díky čemuž mohou vystupovat jako čtyřelektronové donory, ale i jako heterodieny v hetero-Diels-Alderově [4+2] cykloadici. Následující část dokazuje tento předpoklad na reaktivitě C,N chelatovaného fosfinidenu. Diskuze se poté věnuje reaktivitě C,N a N,C,N chelatovaných arsinidenů vůči elektronově chudým alkynům, na což navazuje rozsáhlá studie reaktivity fosfinidenů a arsinidenů vůči *N*-substituovaným maleimidům, přičemž je tato reaktivita diskutována i v porovnání se strukturně blízkými stibinideny a bismutinideny. Poslední část diskuze se zabývá přípravou a reaktivitou arsinidenu chelatovaného nesymetrickým N,C,N ligandem obsahujícím jednu aminovou a jednu iminovou donorovou skupinu. Připravené sloučeniny jsou charakterizovány multinukleární NMR spektroskopií, rentgenostrukturní analýzou, infračervenou a Ramanovou spektroskopií, hmotnostní spektrometrií, elemetnární analýzou a měřením bodu tání.

Klíčová slova

Fosfor, arsen, chelatující ligand, pniktiniden, 2,1-benzazapniktol, hetero-Diels-Alderova cykloadice, koordinační sloučeniny

Table of Contents

1 Introduction

For a recently discovered N,C,N chelated phosphinidene **A**, an interesting property was described,[1] which also is apparent for an analogous N,C,N chelated arsinidene **B**.[2] As seen from their molecular structures, the central atom is not coordinated by both of the imino groups. In solution, however, the ligands appear to be symmetrical as already established for heavier N,C,N chelated compounds containing antimony or bismuth **C** and **D**.[3] Thus a dynamic process involving the central atom was described and called "bell-clapper" fluxionality, which means that the central atom migrates quickly between both of the nitrogen atoms. Looking at the discrete forms the molecules can assume (Figure 1), it can be concluded that while in the symmetrical pnictinidene form, the central atom is formally monovalent. However, the non-symmetrical structure contains the central atom in an oxidation state +III and therefore can be considered a heterocyclic $\sigma^2 \lambda^3$ 2,1-benzazapnictol. This line of thought was the basis for a literary research into the topics of pnictinidenes and several heteropnictoles.

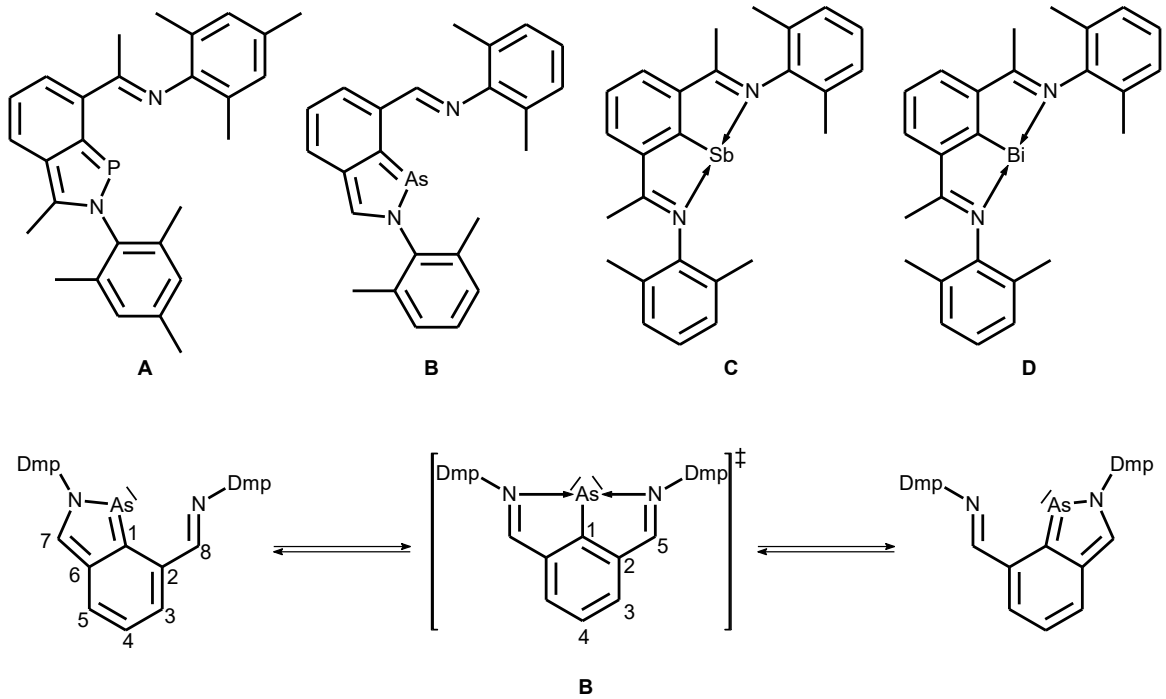

*Figure 1. Structures of compounds **A** – **D** and the "Bell-clapper" behaviour of compound **B***

In the area of pnictinidene chemistry, phosphinidenes have been studied to the greatest degree. Despite this, there has been only a single report of a monomeric phosphinidene stabilised without the use of a Lewis acid or base, solely by the use of a sterically demanding carbene.[4] Going down the Group 15, heavier pnictinidenes have been largely omitted in comparison, both concerning their preparation and reactivity. Notable results in regards to this work include the preparation of N,C,N chelated monomeric compounds containing phosphorus[1], arsenic[2], antimony and bismuth,[3,5] as well as the use of an N,C,N chelated bismuthinidene as a catalyst.[6,7]

On the other hand, barely any results can be found on the topic of 2,1-arylheteropnictoles, with a 2,1-benzazaphosphole **1** compound being the only relevant example known to date, which was also obtained as an unexpected product.[8]

Based on the research of the current state of the topic, the goals of this thesis were set:

1) Preparation of C,N and N,C,N chelated pnictinidenes containing phosphorus or arsenic as central atoms
2) Characterisation of the new C,N and N,C,N chelated pnictinidenes, taking their σ^2 λ^3 2,1-benzazaapnictol character into account.
3) Exploration of the reactivity of the new C,N and N,C,N chelated pnictinidenes
4) Characterisation of acquired products

2 Results and Discussion

2.1 Bonding Situation in Pnictinidenes and the Reasons for the Preparation of 2,1-benzazapnictols

The above-mentioned attribute of central atoms in **A** and **B** being coordinated by only a single nitrogen atom was further corroborated by a theoretical study, which describes the symmetrical arsinidene form of **B** (Figure 1) as an excited state representing only a low activation barrier ($\Delta G^{\ddagger}$= 1.7 kcal/mol) in the process of migrating the arsenic atom between both imino groups. According to NICS calculations, the five-membered C_3NAs ring in **B** exhibits relatively high degree of aromaticity ($NICS(1)_{zz}$ = -25.2 ppm), which is comparable to **A** ($NICS(1)_{zz}$ = -26.8 ppm), but significantly more aromatic than **C** ($NICS(1)_{zz}$ = -8.8 ppm) and **D** ($NICS(1)_{zz}$ = -7.3 ppm). These results further support the claim that **B** can be viewed as a heterocyclic σ^2 λ^3 2,1-benzazaarsole.

Considering these conclusions, the possibility of preparing 2,1-benzazaphosphole and arsole based on a C,N skeleton instead of the discussed N,C,N ligands was the next logical step.

Therefore, a starting aryl-bromide precursor was lithiated, reacted with phosphorus(III) or arsenic(III) chloride and finally reduced using magnesium to give products **1**[8] and **2** (Figure 2). Both compounds were characterized by ^1H and $^{13}C\{^1H\}$ NMR spectroscopy, showing one set of signals containing typical signals assigned to imino group H7 (**1**: $\delta(^1H)$= 7.58 ppm; **2**: $\delta(^1H)$ = 7.89 ppm) and C7 atoms (**1**: $\delta(^{13}C\{^1H\})$ = 135.9 ppm; **2**: $\delta(^{13}C\{^1H\})$ = 141.8 ppm). $^{31}P\{^1H\}$ NMR spectrum shows a signal for compound **1** at 182.1 ppm.

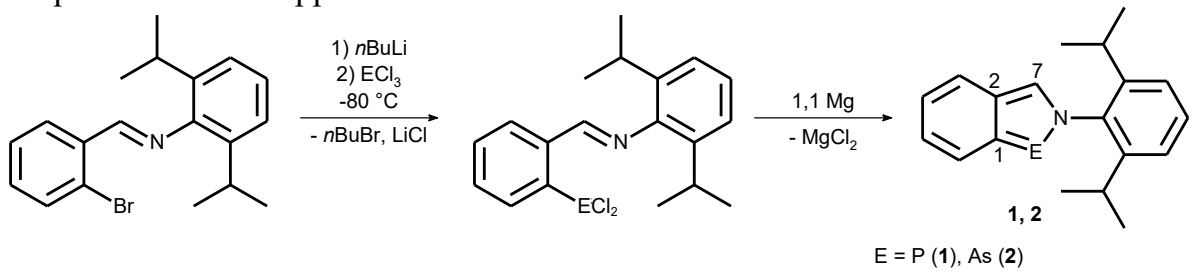

*Figure 2. Preparation of **1** and **2***

Crystal structures of **1**[8] and **2** (Figure 3) show planar monomeric molecular structure with distances P1-N1 (1.702(10) Å) and As1-N1 (1.883(6) Å), which are noticeably shorter compared to the corresponding bond lengths of **A** (1.757(2) Å) and **B** (1.925(5) Å) indicating a possible increase in aromaticity of the five-membered ring in

1 a **2**, which is indeed supported by a NICS study, where both **1** ($NICS(1)_{zz}$ = -31.9 ppm) and **2** ($NICS(1)_{zz}$ = -29.4 ppm) display more negative values compared to **A** and **B**.

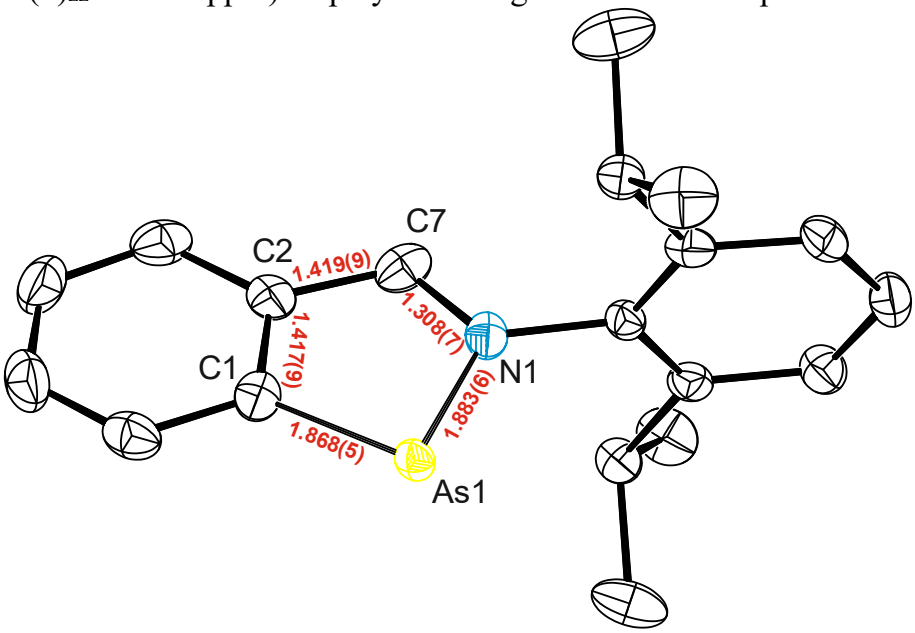

*Figure 3. Molecular structure of **2** including selected distances*

Thus, a reasonable basis for the understanding of the existence of two significant forms the N,C,N chelated arsinidene **B** can exist in has been established. Furthermore, a new 2,1-benzazaarsole **2** was prepared as well as the already observed 2,1-benzazaphosphole **1**[8] was purposefully prepared using a novel approach.

2.2 **Reactivity of Compound** 1

Further, the reactivity of the prepared **1** had been explored. Looking at the resonance structures of a model compound **1'** obtained by the means of the NRT method (Figure 4), there are only two meaningful forms to be considered. One of them depicts **1'** as a heterocyclic 2,1-benzazaphosphole (**1'A**), while the other shows **1'B** to be a zwitterionic structure with two electron pairs located at the phosphorus atom. Therefore compound **1** was used to probe both border forms. The heterocyclic structure offers an interesting way of manifesting itself as a heterodiene in [4+2] cycloadditions. The zwitterionic structure offers on the other had up to two electron pairs for the coordination of transition metals in a similar manner the phosphinidene **1'C** might. These assumptions are also supported by theoretical NBO calculations.

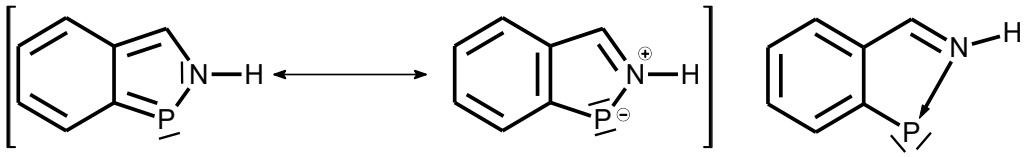

1'A 17,1 % **1'B** 12,5 % **1'C**

*Figure 4. Resonance structures of **1'***

Compound **1** was therefore first of all treated with electron-deficient alkynes, namely with dimethyl acetylenedicarboxylate (DMAD) and (tetrafluoro-4-pyridyl)ethyne to give compounds **3** and **4** respectively as yellow crystals (Figure 5).

Both compounds were characterized by X-ray crystallography. The molecular structures (Figure 6 for **3**) show that these reactions gave the products of the hetero-Diels-Alder cycloaddition through the formation of two new bonds, specifically P1-C9 (**3**: 1.904(2) Å; **4**: 1.897(2) Å) and C7-C8 (**3**: 1.545(2) Å; **4**: 1.557(3) Å).

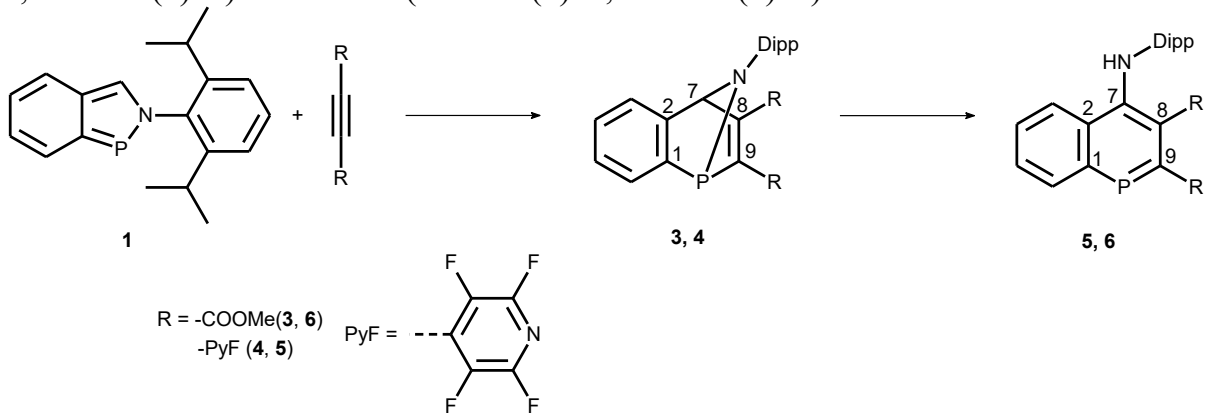

*Figure 5. Preparation of **3** – **6***

^{1}H and $^{13}C\{^{1}H\}$ NMR spectra show a change in the chemical shifts in compounds **3** and **4** in comparison with the starting compound **1**. Most notably, the signal representing *H*7 (**3**: $\delta(^{1}H) = 5.64$ ppm; **4**: $\delta(^{1}H) = 5.26$ ppm) as well as the respective *C*7 signal (**3**: $\delta(^{13}C\{^{1}H\}) = 82.4$ ppm; **4**: $\delta(^{13}C\{^{1}H\}) = 84.4$ ppm) are shifted toward higher fields (*cf.* for **1** $\delta(^{1}H) = 7.58$ ppm; $\delta(^{13}C\{^{1}H\}) = 135.9$ ppm). Similarly, the $^{31}P\{^{1}H\}$ NMR spectra depict signals of both compounds (**3**: $\delta(^{31}P\{^{1}H\}) = 39.9$ ppm; **4**: $\delta(^{31}P\{^{1}H\}) = 40.7$ ppm) significantly high-field shifted in contrast with **1** ($\delta(^{31}P\{^{1}H\}) = 182.1$ ppm).

IR and Raman spectra show two bands in the range 1729 – 1707 cm^{-1}, thus further confirming the presence of carbonyl groups in **3**. A band assigned to the C8=C9 bond is visible in the Raman spectrum at 1610 cm^{-1}. Regarding **4**, carbonyl bands are located at 1645 and 1464 cm^{-1} and the C8=C9 vibration is found at 1614 cm^{-1}.

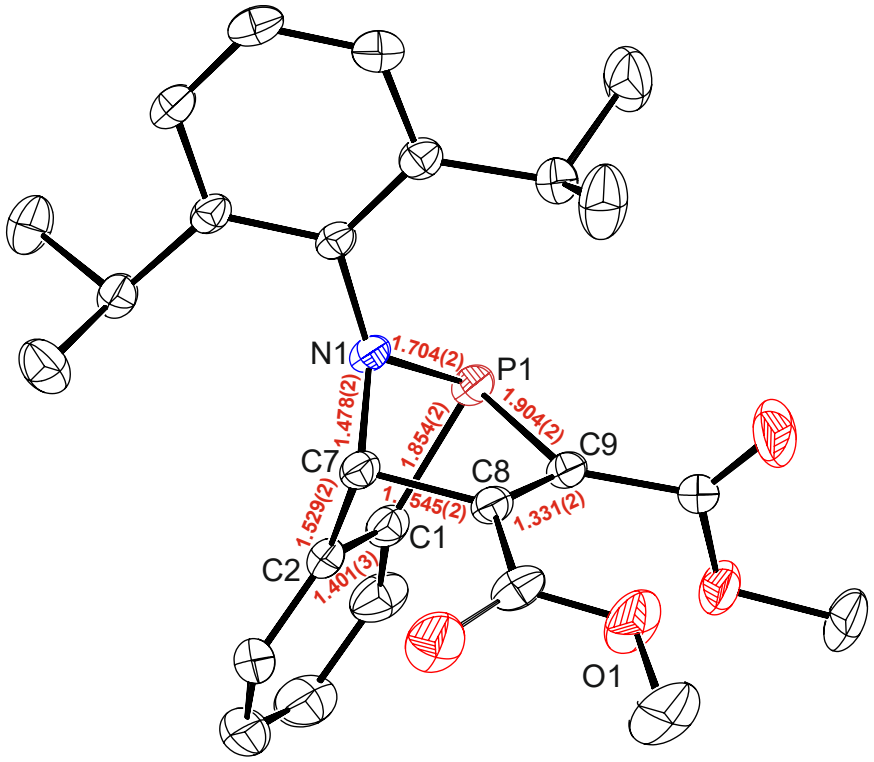

*Figure 6. Molecular structure of **3** including selected distances*

Compound **4** was heated up to 120 °C in toluene and quite an interesting reaction took place, where a proton migration allowed for the cleavage of the P1-N1 bond and the aromatization of the remaining six-membered C_5P ring, affording a derivative of a 1-phosphanaphthalene **5** (Figure 5). Analogous reaction was subsequently attempted with **3**. The same approach (i.e. heating in toluene) was ineffective due to significantly longer reaction times and the occurrence of side reactions. Therefore, pyridine as a proton-transferring agent was introduced as a solvent, which then offered **6** at much lower temperatures and shorter reaction times (Figure 5).

Compound **5** was characterized by X-ray crystallography (Figure 7) showing the bond P1-N1 in **4** being cleaved. The resulting molecular structure shows a nearly planar geometry for the condensed rings, exhibiting bond lengths P1-C1 (1.755(4) Å) and P1-C9 (1.713(5) Å).

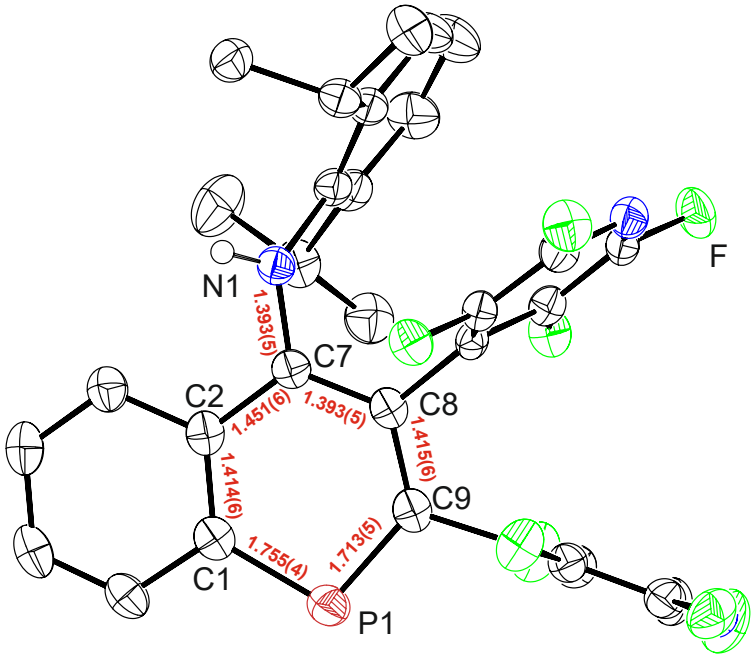

*Figure 7. Molecular structure of **5** including selected distances*

The ^{1}H and $^{13}C\{^{1}H\}$ NMR analysis carried out for **5** and **6** show a signal assigned to the amino group N*H* hydrogen (**5**: $\delta(^{1}H)$ = 6.16 ppm; **6**: $\delta(^{1}H)$ = 9.22 ppm), the existence of which was further supported by the means of a ^{1}H, ^{15}N HMBC experiment showing doublets (^{15}N ~ -298 ppm) with coupling constants $^{1}J(^{15}N, ^{1}H)$ ~ 91 Hz. Furthermore, $^{31}P\{^{1}H\}$ NMR spectra depicted one signal for **5** ($^{31}P\{^{1}H\}$ = 165.1 ppm) and **6** ($^{31}P\{^{1}H\}$ = 168.3 ppm).

IR and Raman spectroscopy also shows a band assigned to N-H vibration at 3436 and 3293 cm^{-1}.

During crystallization attempts of **6**, an accidental hydrolysis took place, which gave single crystals of **7** (Figure 8), which were characterized by X-ray crystallography (Figure 9). A new bond between P1-P1a (2.209(7) Å) was observed. At the same time, a new bond P1-O1 (1.426(1) Å) was formed and the carbon atom C9 became sp^3 hybridized.

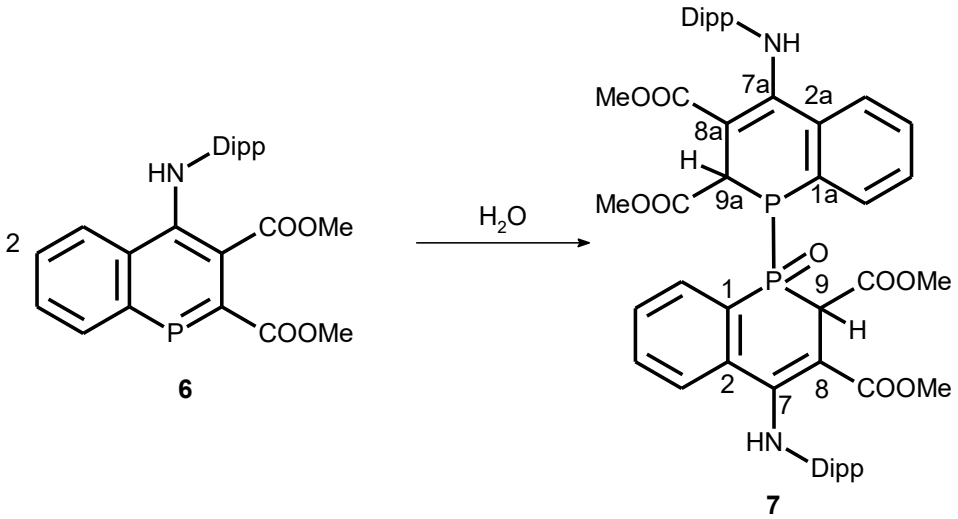

*Figure 8. Hydrolysis of **6***

NMR analysis gave $^{31}P\{^{1}H\}$ spectra showing two phosphorus doublets representing *P*P=O ($\delta(^{31}P\{^{1}H\})$ = -42.6 ppm) and P*P*=O groups ($\delta(^{31}P\{^{1}H\})$ = 32.3 ppm), both being coupled with $^{1}J(^{31}P, ^{31}P)$ = 264 Hz. ^{1}H NMR spectra show two signals for the two N*H* hydrogen atoms ($\delta(^{1}H)$ = 11.45; 11.80 ppm), which are also coupled with ^{15}N atoms (δ (^{15}N ~ 279 ppm, $^{1}J(^{15}N, ^{1}H)$ = 89 Hz). Signals for *HC*9 and *HC*9a are also visible ($\delta(^{1}H)$ = 4.63; 4.73 ppm), ($\delta(^{13}C\{^{1}H\}$ = 34.9; 45.3 ppm).

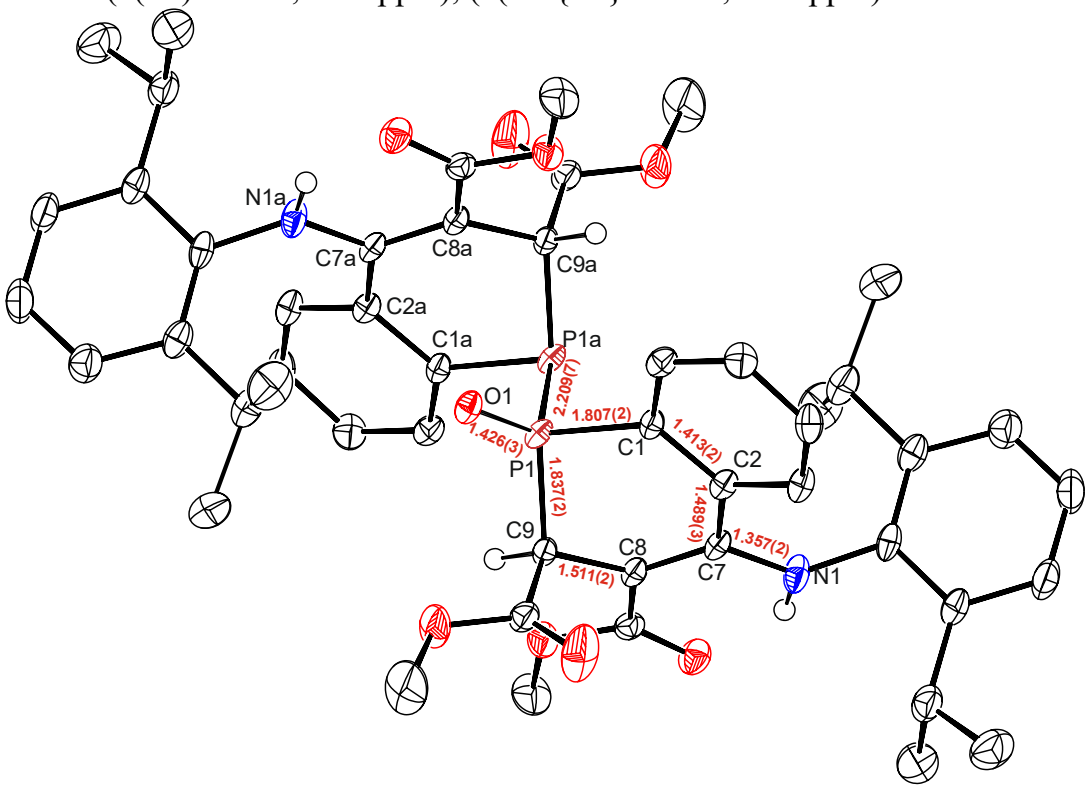

*Figure 9. Molecular structure of **7** including selected distances*

IR and Raman spectroscopy depicts a band of the carbonyl groups at 1735 cm^{-1} as well as a P=O vibration is observable at 1201 cm^{-1}.

To reinforce the above-described results, **1** was treated with several *N*-substituted maleimides, which act as dienophiles by offering their double bond to the cycloaddition. Reaction of **1** with maleimides thus led to the formation of cycloadducts **8** – **10** (Figure 10).

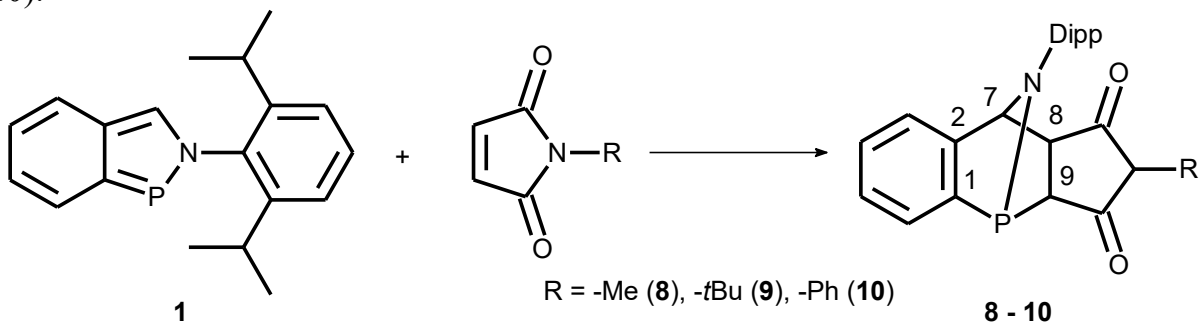

*Figure 10. Preparation of **8** – **10***

Single crystals of **8** and **10** were characterized using X-ray crystallography (Figure 11), revealing the cycloaddition gave similar products to those mentioned above, as two new bonds P1-C9 (1.904(4) Å (**8**); 1.912(2) Å (**10**)) and C7-C8 (1.562(5) Å (**8**) a 1.581(1) Å (**10**)) can be observed.

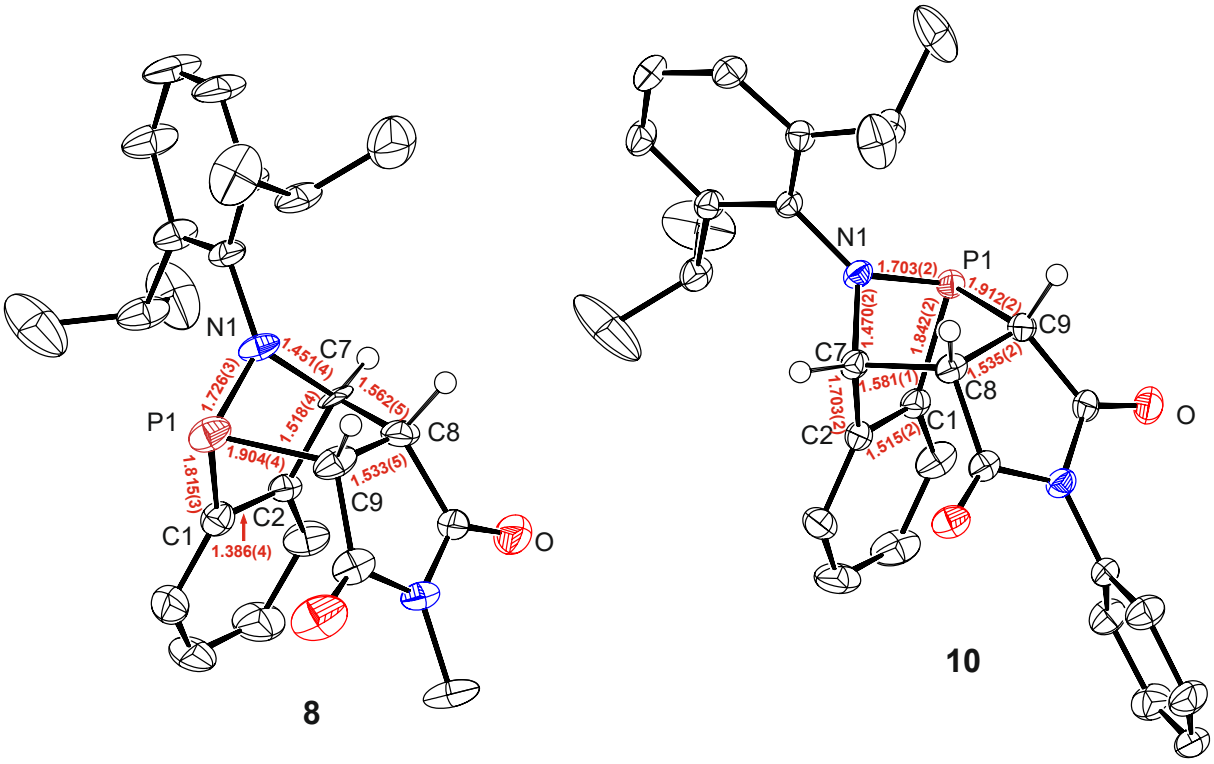

*Figure 11. Molecular structure of **8** and **10** including selected distances*

^{1}H NMR analysis shows an ABX spin system which includes signals corresponding to *H*7, *H*8 and *H*9 atoms. ^{31}P{^{1}H} spectra show similar chemical shifts for the phosphorus atoms of each compound (^{31}P{^{1}H} = 31.6 – 33.0 ppm).

IR and Raman spectra show two bands at 1766 and 1697 cm^{-1} related to vibrations of the carbonyl groups.

Proving **1** can act as a heterodiene, next the task was to test whether it can also serve as a ligand for transition metals. First, a reaction with two equivalents of chloro(dimethylsulfide)gold(I) complex was carried out, obtaining a yellow precipitate **11** (Figure 12). The product was isolated as single crystals and was characterized by X-ray crystallography (Figure 13), revealing its molecular structure to consist of two molecules interacting via Au-Au aurophilic interactions (3.2613(6) and 3.3628(7) Å). Moreover, in both molecules the phosphorus atom is acting as a four-electron donor for two AuCl moieties (2.216(3)-2.235(3) Å).

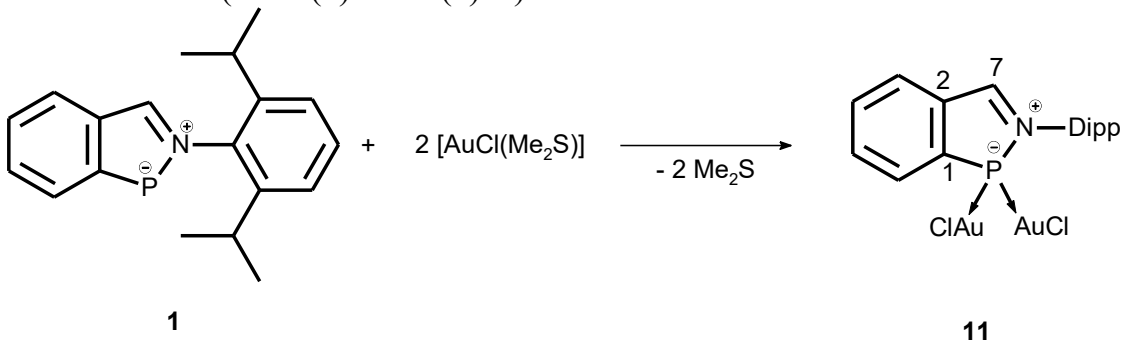

*Figure 12. Preparation of **11***

Despite the low solubility of **11**, ^{1}H and ^{31}P{^{1}H} NMR spectra could be obtained. In ^{1}H NMR spectrum, a C*H*N group is visible (δ(^{1}H) = 8.78 ppm), while ^{31}P{^{1}H} spectrum shows one signal at 140.1 ppm.

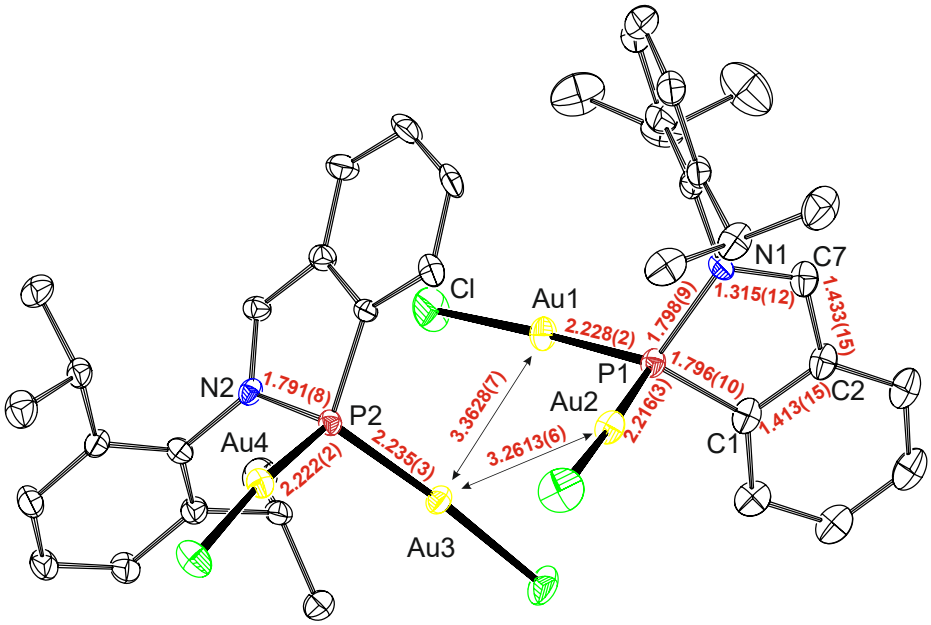

*Figure 13. Molecular structure of **11** including selected distances*

Next, **1** reacted with one equivalent of silver triflate and silver tetrafluoroborate. These reactions afforded lightly coloured precipitates of **12** and **13** (Figure 14) and after crystallization, compound **12** was characterised by X-ray crystallography.

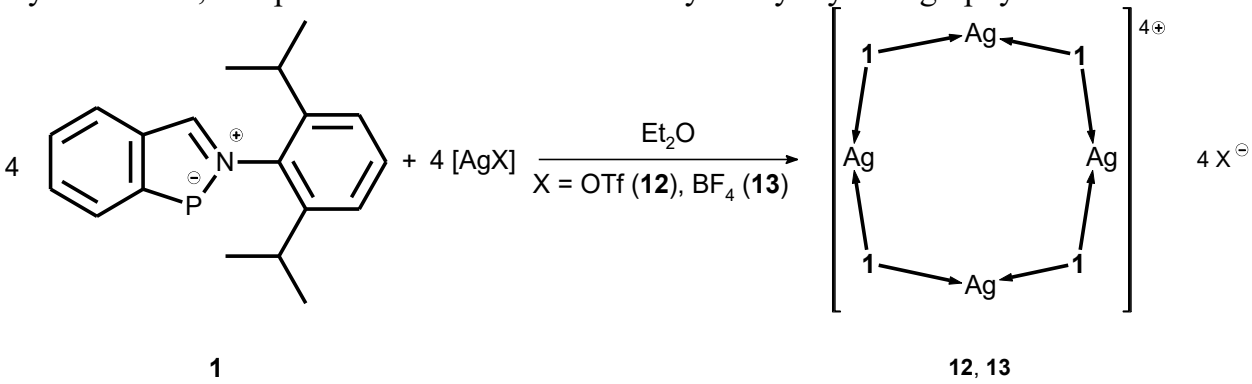

*Figure 14. Preparation of **12** and **13***

It was observed that **12** is formed as a tetramer making up a cycle in which each silver atom is coordinated by two phosphorus atoms and each phosphorus atom coordinates two silver atoms (P-Ag 2.432(3) – 2.451(3) Å), thus again acting as a four-electron donor (Figure 15).

NMR spectra of **12** and **13** show signals of common atoms at rather similar chemical shifts, which leads to conclusion that in solution, the different anions (triflate vs tetrafluoroborate) do not affect their structures significantly.

ESI-MS spectrometry performed for **12** in acetonitrile revealed ion fragments containing up to four silver atoms, thus suggesting the tetrameric structure is retained in solution.

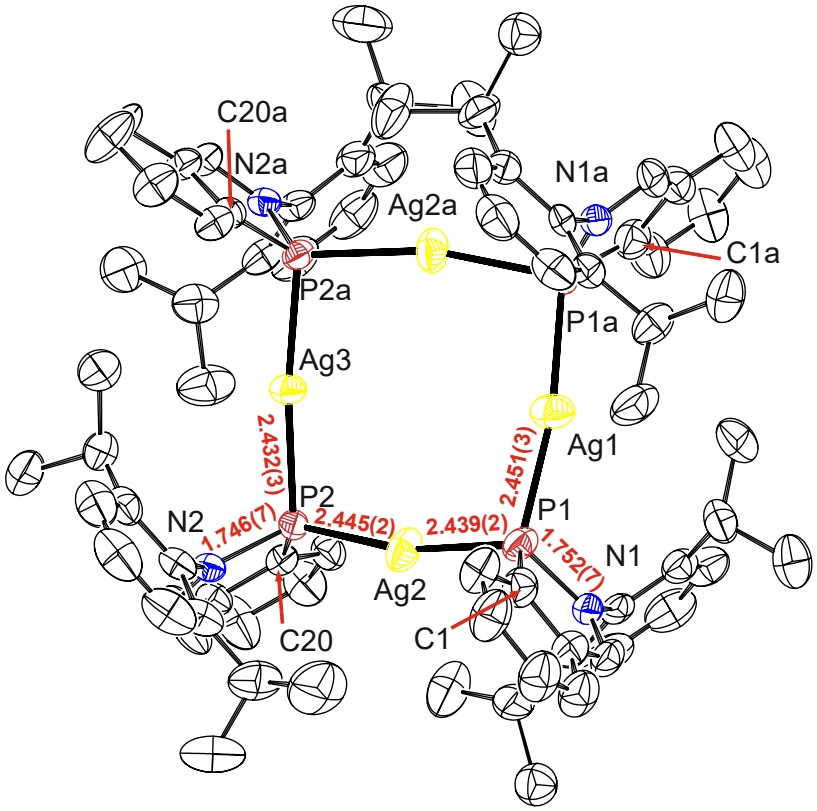

*Figure 15. Molecular structure of **12** including selected distances*

Finally, starting **1** was treated with an equivalent of dicobalt octacarbonyl. While eliminating carbon monoxide, product **14** was formed and turned the reaction mixture dark blue (Figure 16). After workup, the compound was characterized by X-ray crystallography. It shows the phosphorus atom serving as a ligand for two atoms of cobalt (P-Co 2.118(6); 2.139(6) Å) (Figure 17).

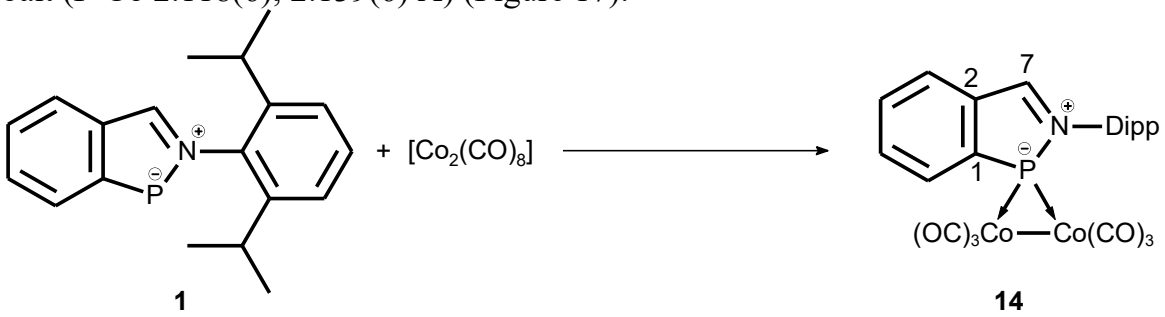

*Figure 16. Preparation of **14***

^{1}H and ^{13}C{^{1}H} NMR spectroscopy shows signals for *H*7 (δ(^{1}H) = 9.32 ppm) and *C*7 (δ(^{13}C{^{1}H}) = 166.3 ppm) as well as for *C*O (δ(^{13}C{^{1}H}) = 206.3 ppm) moieties. ^{31}P{^{1}H} signal can be found at 265.6 ppm.

The presence of the carbonyl ligands was also confirmed by the means of IR spectroscopy, where six strong bands can be seen (2043, 1998, 1987, 1961, 1951 and 1932 cm^{-1}). In solution only three bands were observed (2046, 2005 and 1978 cm^{-1}).

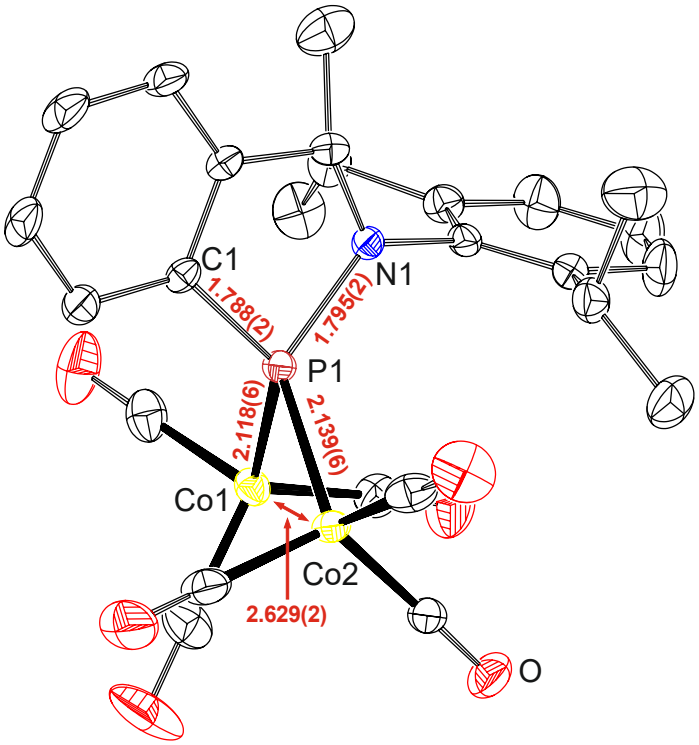

*Figure 17. Molecular structure of **14** including selected distances*

The previous accounts of reactivity of **1** show its tendency to act as both heterodiene and four-electron donor toward several transition metals.

2.3 Heterodiene Character of 2,1-benzazaarsoles

The following paragraphs are summarizing the reactivity of several 2,1-benzazaarsole derivatives. In particular, first the previously mentioned **2** (Figure 2) will be discussed followed by the reactivity of **B**[2] (Figure 1) and concluding with a newly prepared compound.

Compound **15** was prepared by the lithiation of a bromo-substituted ligand-precursor, subsequent treatment with $AsCl_3$, the intermediate was reduced using KC_8 (Figure 18).

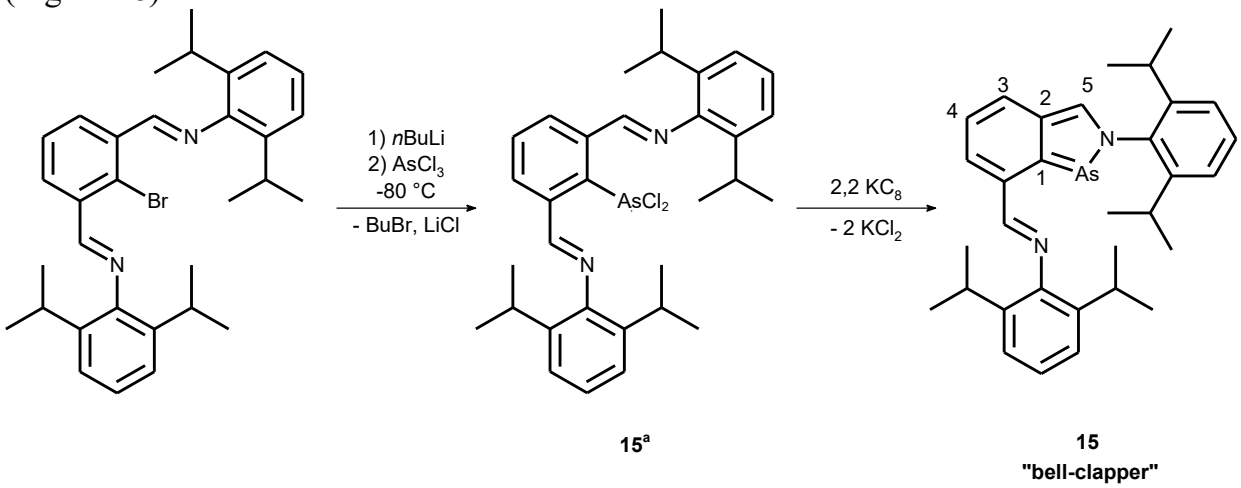

*Figure 18. Preparation of **15***

X-ray molecular structure (Figure 19) shows particularly the different distances between As1-N1 (1.933(3) Å) and As1-N2 (2.469(6) Å), indicating the structure of 2,1-benzazaarsole.

^{1}H and ^{13}C{^{1}H} NMR spectra depict most importantly the signals of *H*5 (δ(^{1}H) = 8.35 ppm) and *C*5 (δ(^{13}C{^{1}H}) = 152.8 ppm).

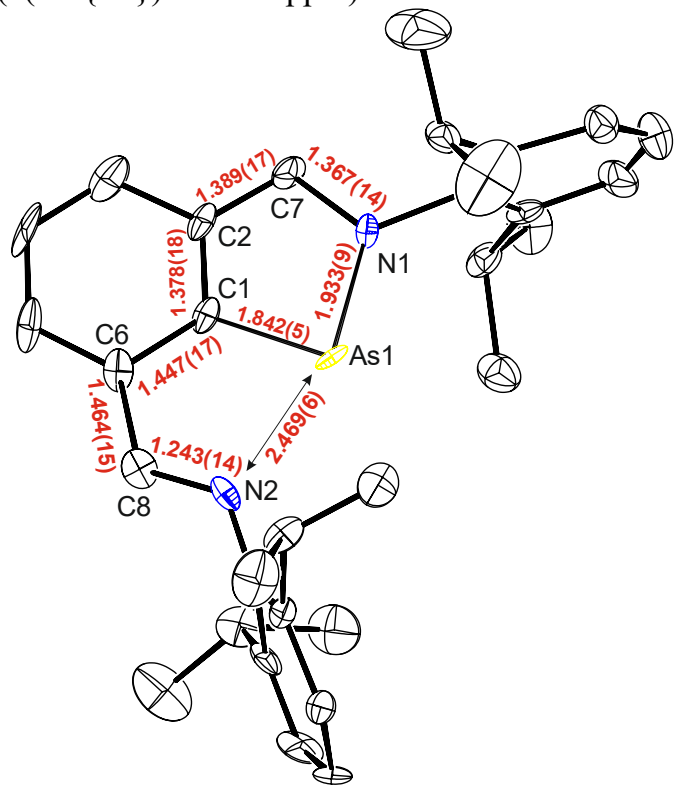

*Figure 19. Molecular structure of **15** including selected distances*

Now starting at the beginning, the precursor **2** was first treated with DMAD, offering under strict conditions product **16** (Figure 20). It was characterized using X-ray diffraction analysis, showing a cycloaddition occurred and thus two bonds As1-C9 (2.045(5) Å) and C7-C8 (1.546(8) Å) were formed.

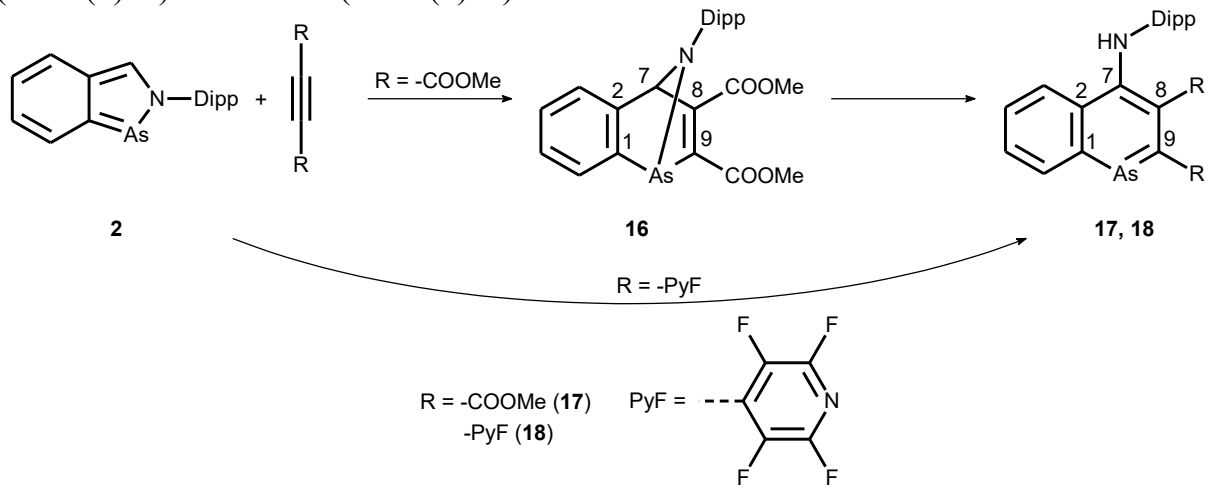

*Figure 20. Preparation of **16** – **18***

NMR spectra of **16** display characteristic chemical shifts of *H*7 (δ(^{1}H) = 5.92 ppm) and *C*7 (δ(^{13}C{^{1}H}) = 84.6 ppm) as well as *C*8 (δ(^{13}C{^{1}H} = 164.0 ppm) and *C*9 (δ(^{13}C{^{1}H} = 153.4 ppm).

Two bands in IR and Raman spectra at 1722 and 1707 cm^{-1} were assigned to the carbonyl moieties vibrations. The presence of C8=C9 double bond was also supported by a band at 1613 cm^{-1} in the IR spectrum.

Dissolving of **16** in benzene smoothly led to the formation of product **17** (Figure 20). X-ray crystallography confirmed the molecular structure of **17** to be a derivative of 1-arsanaphthalene. The cleavage of the As1-N1 bond is apparent as well as the proton transfer from C7 to N1. The C-C distances of the naphthalene rings are between the margins of (1.369(2) – 1.442(2) Å) and the angle C1-As1-C9 is equal to 96.57(7)°.

17 was also analysed using NMR spectroscopy. It showed characteristic signals for the N*H* amino group ($\delta(^1H)$ = 8.49 ppm) and was further confirmed by ^1H, ^{15}N HMBC experiment which showed a doublet belonging to the nitrogen atom ($\delta(^{15}N)$ = -294 ppm; $^1J(^{15}N, ^1H)$ = 89 Hz).

The presence of NH group was further corroborated by the band at 3288 cm^{-1} visible in IR and Raman spectra.

As another dienophile, bis(2,3,5,6-tetrafluoro-4-pyridyl)ethyne was used. Reaction with **2** led to the formation of the product **18** (Figure 20), which was unambiguously characterized as another 1-arsanaphthalene derivative by X-ray crystallography showing C-C distances in the naphthalene cycles (1.360(4) – 1.447(3) Å) and the C1-As1-C9 angle is 97.40(9)°.

NMR analysis shows N*H* signal ($\delta(^1H)$ = 6.18 ppm) and was further corroborated by an ^1H, ^{15}N HMBC experiment ($\delta(^{15}N)$ = -296 ppm; $^1J(^{15}N,^1H)$ = 89 Hz).

A medium band in IR and Raman spectra with the wavenumber of 3437 cm^{-1} was assigned to the NH group.

For this reaction, the intermediate cycloadduct was not isolated. It was, however, observed in ^1H NMR spectrum of the reaction mixture.

The above-mentioned findings show that **2** is capable of similar reactivity toward dienophiles as the phosphorus analog **1**. The following part is concerned with the compound **B**, which contains a pendant imino group and its inclination to act as a heterodiene might be hampered by the “bell-clapper” fluxionation.

Treatment of **B** with DMAD and bis(2,3,5,6-tetrafluoro-4-pyridyl)ethyne led to the formation of products **19** and **20** (Figure 21). The molecular structure of **20** was determined by X-ray crystallography, showing the product to be a 1-arsanaphthalene derivative, which is also in line with the C-C bond lengths of the annealed cycles (1.363(9) – 1.460(8) Å).

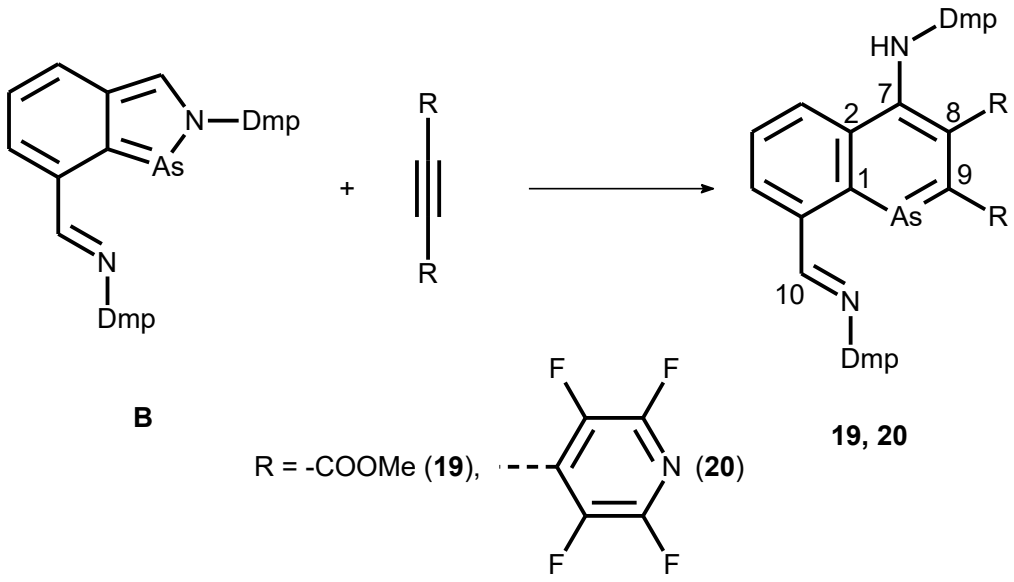

*Figure 21. Preparation of **19** and **20***

^{1}H and ^{13}C{^{1}H} NMR spectra of **19** and **20** showed the signals for the pendant imino group, that is *H*10 (**19** δ(^{1}H) = 8.65 ppm; **20** δ(^{1}H) = 9.28 ppm) and *C*10 in ^{13}C spectra (**19** δ(^{13}C{^{1}H}) = 163.0 ppm; **20** δ(^{13}C{^{1}H}) = 163.6 ppm). Similarly, signals belonging to the amino N*H* moiety can be assigned (**19** δ(^{1}H) = 8.43 ppm; **20** δ(^{1}H) = 5.49 ppm). Furthermore, in the case of **20**, the amino group was also confirmed by ^{1}H, ^{15}N HMBC experiment (δ(^{15}N) = -294 ppm; ^{1}J(^{15}N,^{1}H) = 87 Hz). For **19**, unfortunately, the ^{15}N signal was not observed.

IR and Raman spectra show expected bands for NH group (3316; 3321 cm^{-1}) for **19** and **20** respectively and C=O (1685; 1689 cm^{-1}).

As was the case for **18**, the cycloadduct of **B** with DMAD and bis(2,3,5,6-tetrafluoro-4-pyridyl)ethyne was not successfully isolated.

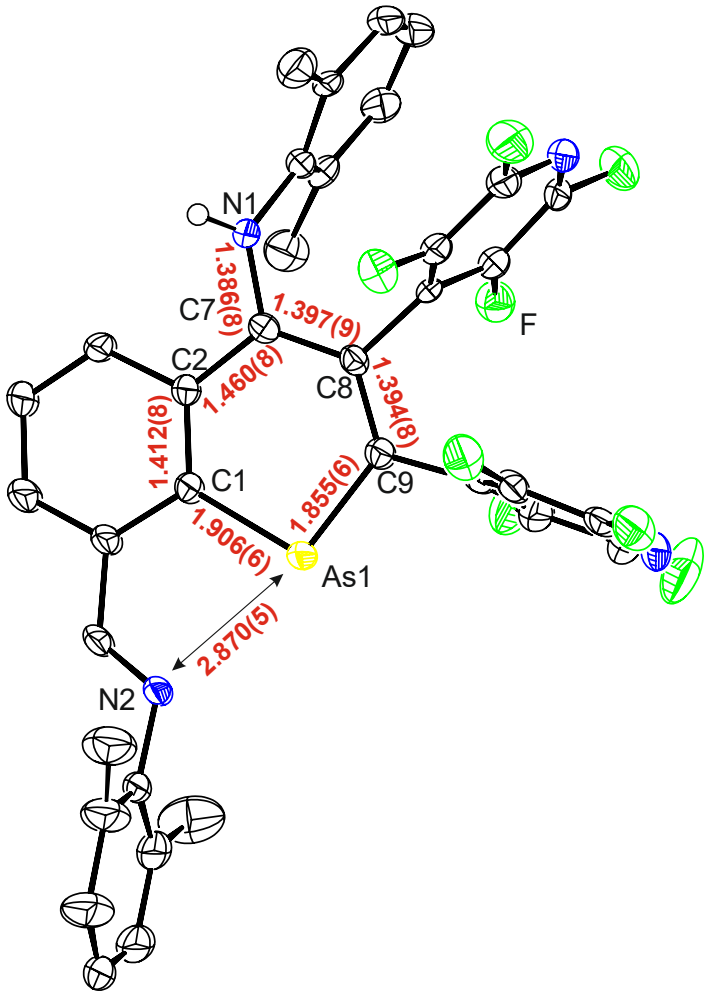

*Figure 22. Molecular structure of **20** including selected distances*

Furthermore, **B** also underwent a reaction with methylpropiolate, i.e. a non-symmetric dienophile. The isolated product **21** (Figure 23) was analysed by X-ray diffraction analysis, thus the molecular structure was obtained. It showed the formation of an1-arsanaphthalene isomer, as illustrated by the C-C bond lengths (1.373(3) – 1.459(3) Å) as only a single isomer.

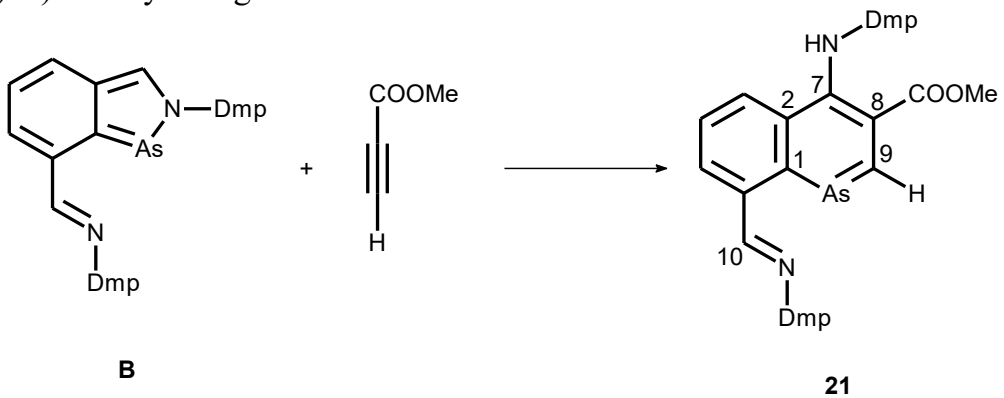

*Figure 23. Preparation of **21***

The ^{1}H and $^{13}C\{^{1}H\}$ NMR data show one set of signals corresponding to **21**. The pendant imino group is observable as singlets *H*10 ($\delta(^{1}H)$ = 9.28 ppm) and *C*10 ($\delta(^{13}C\{^{1}H\})$ = 162.7 ppm). The signal of the amino group is also present ($\delta(^{1}H)$ = 11.41 ppm) as well as the *H*9 signal ($\delta(^{1}H)$ = 10.88 ppm).

Compound **21** was also characterized by IR and Raman spectroscopy, which show bands assigned to N-H (3162; 3165 cm^{-1}) and C=O groups (1668; 1670 cm^{-1}).

These findings lead to conclusion, that **B** can take part in hetero-Diels-Alder reactions as a heterodiene, thus showing similar behaviour to **2**.

Finally, the newly prepared starting compound **15** was also considered. The cycloaddition reactivity of **15** should lead to a good comparison to **2** due to the presence of two -Dipp groups in **15** and one -Dipp substituent in **2**. Also, a steric demand of **15** vs. **B** might be considered.

As a dienophile, DMAD was again the substance of choice. By treating **15** with DMAD, yellow single crystals of **22** were isolated (Figure 24), which were characterized by X-ray crystallography, confirming the molecular structure of a direct cycloadduct. This is illustrated the newly formed bonds As1-C9 (2.013(3) Å) and C7-C8 (1.553(4) Å) and the prevailing As1-N1 bond (1.858(2) Å).

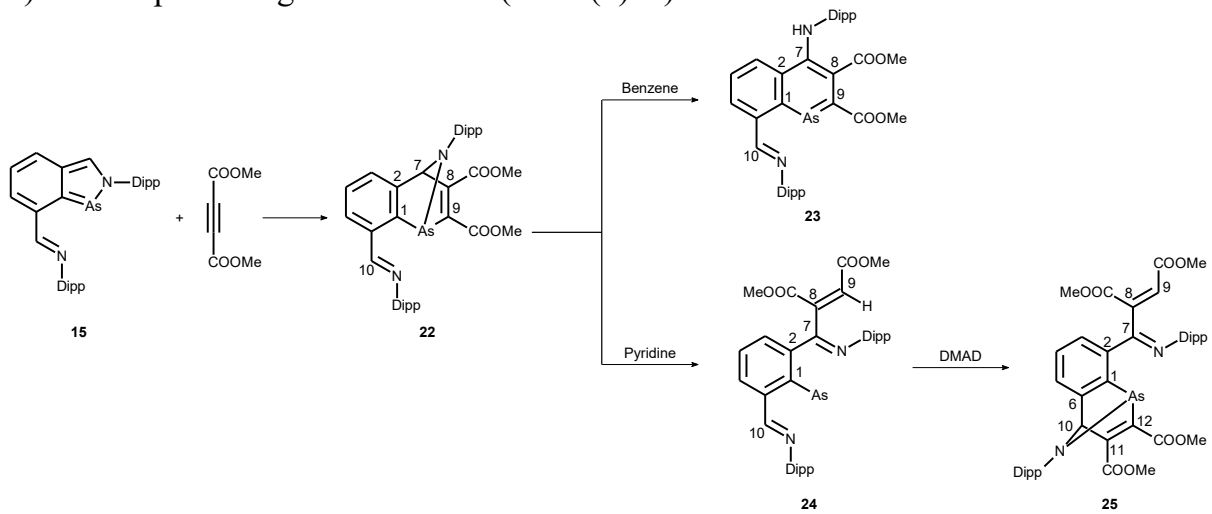

*Figure 24. Preparation of **22** – **25***

^{1}H and $^{13}C\{^{1}H\}$ NMR spectra show one set of signals belonging to **22**. Characteristic singlet signal ($\delta(^{1}H)$ = 6.07 ppm) is assigned to the *H*7 hydrogen and a signal corresponding to *H*10 ($\delta(^{1}H)$ = 8.06 ppm) can be observed as well as the corresponding carbon signals for C7 ($\delta(^{13}C\{^{1}H\})$ = 84.0 ppm) and *C*10 ($\delta(^{13}C\{^{1}H\})$ = 162.8 ppm). Infrared and Raman spectra show C=O bands (1726; 1710 cm^{-1}).

Next, the attempt to transform **22** into a 1-arsanaphthalene was carried out. To that end, two previously successful methods for the preparation of **5** and **6**, specifically heating of the starting compound in benzene and pyridine. First, **22** was heated in benzene to give the target compound **23** (Figure 24).

^{1}H and $^{13}C\{^{1}H\}$ NMR spectra of **23** show N*H* chemical shift ($\delta(^{1}H)$ = 9.39 ppm) as well as *C*7 ($\delta(^{13}C\{^{1}H\})$ = 149.4 ppm). The signal corresponding to the free imino group hydrogen *H*10 is visible ($\delta(^{1}H)$ = 8.80 ppm). Vibrational spectroscopy shows a band assigned to N-H bond (3390 cm^{-1}).

The second method involved dissolving **22** in pyridine and heating the mixture up. As opposed to similar approach leading to the 1-phosphanaphthalene derivative **6**, in this reaction **24** was isolated instead (Figure 24) in the form of purple crystals.

^{1}H NMR spectra show the signals for *H*9 ($\delta(^{1}H)$ = 6.77 ppm) and *H*10 ($\delta(^{1}H)$ = 8.38 ppm). In $^{13}C\{^{1}H\}$ NMR spectra *C*9 ($^{13}C\{^{1}H\}$ = 129.7 ppm) and *C*10 ($\delta(^{13}C\{^{1}H\})$ =

158.7 ppm) can be observed. In the IR and Raman spectra, a band belonging to the C=O bond can be found at 1727 or 1739 cm^{-1} respectively.

Due to the bonding situation on the arsenic atom in **24** being similar to the starting compound **15**, a possibility of another cycloaddition was considered by adding a second equivalent of DMAD to **24**, leadings to the formation of **25** (Figure 24). Its molecular structure was obtained by X-ray diffraction analysis (Figure 25), which confirmed the second hetero-Diels-Alder reaction taking place by the formation of two new bonds As1-C12 (2.015(7) Å) and C10-C11 (1.542(10) Å).

^{1}H and $^{13}C\{^{1}H\}$ NMR spectra show signals corresponding to the newly formed compound **25**. Most importantly, the signals for *H*10 ($\delta(^{1}H)$ = 5.95 ppm) and *C*10 ($\delta(^{13}C\{^{1}H\})$ = 83.5 ppm) are visible. In the vibrational spectra, three bands assigned to the C=O bonds can be seen at 1736, 1726 and 1715 cm^{-1}.

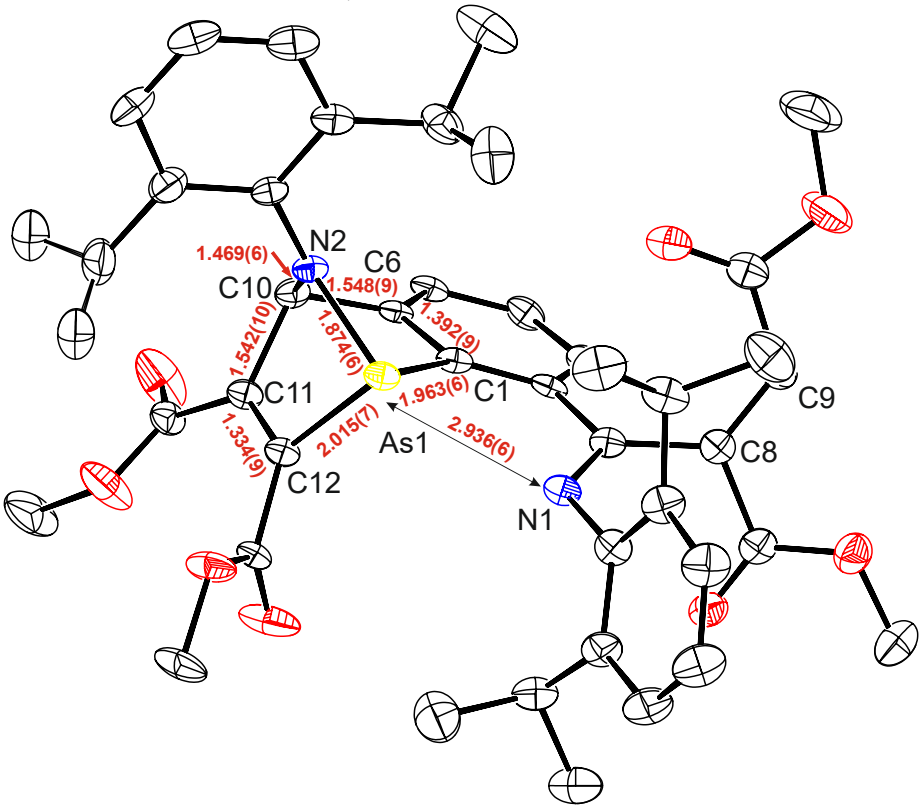

*Figure 25. Molecular structure of **25** including selected distances*

Above, the tendency of three 2,1-benzazaarsoles to react as heterodienes was discussed. It was established that all considered starting compounds can react this way and afford their corresponding 1-arsanaphthalene derivatives as well. Interesting outlier behaviour of the compound **22** derived from **15** in pyridine was also described giving **24**, which can react with a second equivalent of DMAD to give **25**.

2.4 Reversibility of the Cycloaddition Reactions Involving 2,1-benzazapnictoles and Maleimides

A preliminary study concerning the cycloaddition reactions of a stibinidene **E** with *N*-substituted maleimides has shown an exceptional tendency to give the starting compounds upon heating the solutions of the isolated products **E1** – **E3** (Figure 28A).[9] The following chapter expands on this study and includes various 2,1-benzazaphospholes and arsoles in reactions with maleimides, the focus being the

reversibility of these reactions. The entire study also considers several starting compounds containing antimony and bismuth, which are mentioned here to relate the findings in the scope of the whole Group 15, however their characterization is not included, as these compounds are not a part of this thesis. Moreover, the already published **E1** – **E3** and the above-mentioned **8** – **10** derived from **1** are included.

To study their reactivity, three groups of starting compounds were prepared. Two N,C,N pincer ligand derivatives were used to assess the influence of different imino substituents (-tBu vs -Dmp), as well as a C,N chelating ligand to compare how a pendant imino moiety affects the reaction (Figure 26).

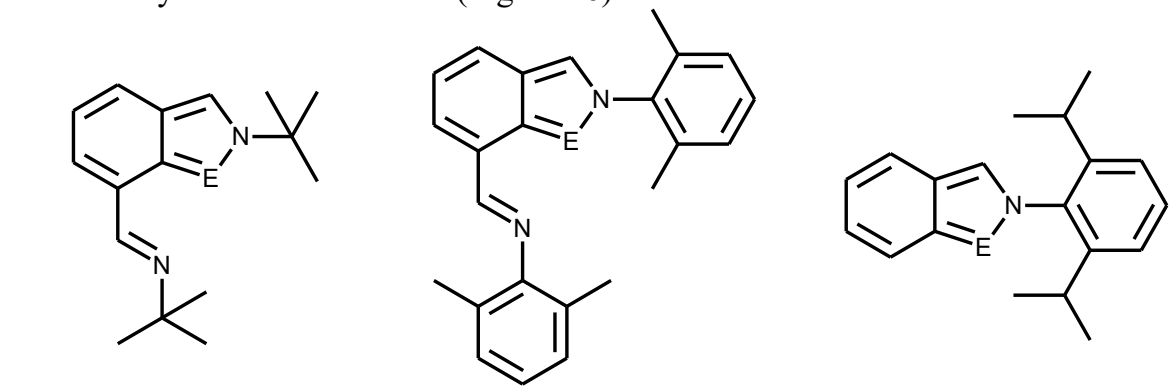

Figure 26. Overview of the starting compounds to be treated with N*-substituted maleimides*

The starting **B**[2], **F**[10], **G**[5], **H**[11] were prepared according to literature, while two new phosphorus compounds **26** and **27** were prepared by the lithiation of the respective bromo-substituted precursor and subsequent reaction with phosphorus(III) chloride followed by the reduction using magnesium (Figure 27).

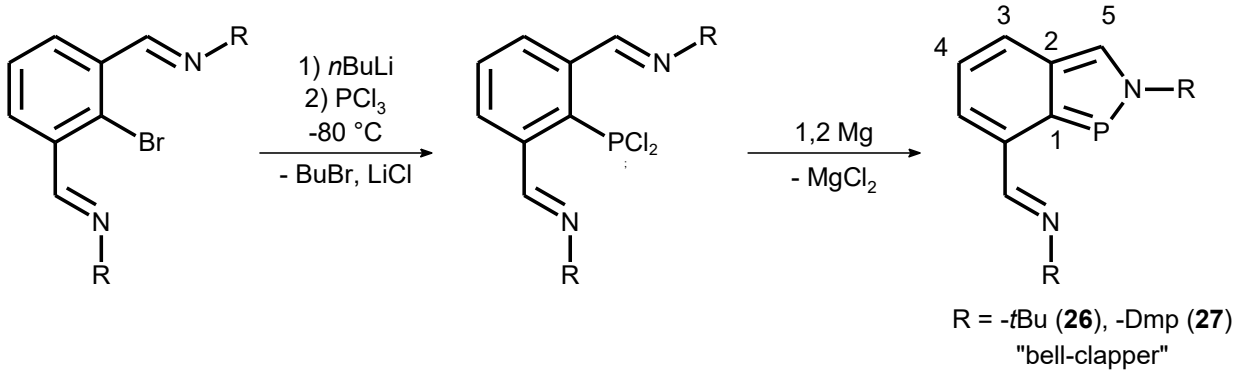

*Figure 27. Preparation of **26** and **27***

Both isolated compounds were characterized by ^{1}H and $^{13}C\{^{1}H\}$ NMR spectroscopy, where the signals belonging to *H*5 ($\delta(^{1}H)$ = 8.27 (**26**); 7.77 (**27**) ppm) and *C*5 ($\delta(^{13}C\{^{1}H\})$ = 143.1 (**26**); 148.9 (**27**) ppm) located on the imino function can be seen. Phosphorus NMR spectra also show one signal for each compound ($\delta(^{31}P\{^{1}H\})$ = 162.3 (**26**); 171.8 (**27**) ppm).

Subsequently, each of the starting compounds was treated with three *N*-substituted maleimides (-Me, -*t*Bu, -Ph). Most of the products were isolated as white crystalline material. Compounds **8** – **10** were characterised above, while **E1** – **E3** were discussed in literature.[9]

Starting compounds **2**, **26**, **27** and **G** reacted smoothly with all three maleimides, affording expected cycloaddition products (Figure 28A). Compounds **28**, **30**, **31**, **32**, **40** and **41** were characterised by X-ray crystallography, revealing similar structure to **8** and **10**. It also showed that the starting 2,1-benzazapnictole affected the stereoselectivity of the reaction, giving either exo- (**28**, **30**, **31** and **32**) or endo- (**40**, **41**) isomers. For the exo- isomer, the torsion angles of HC7-C8H are between 71 – 78°, while the endo-isomers show sharper angles between 42 – 49° (Figure 29).

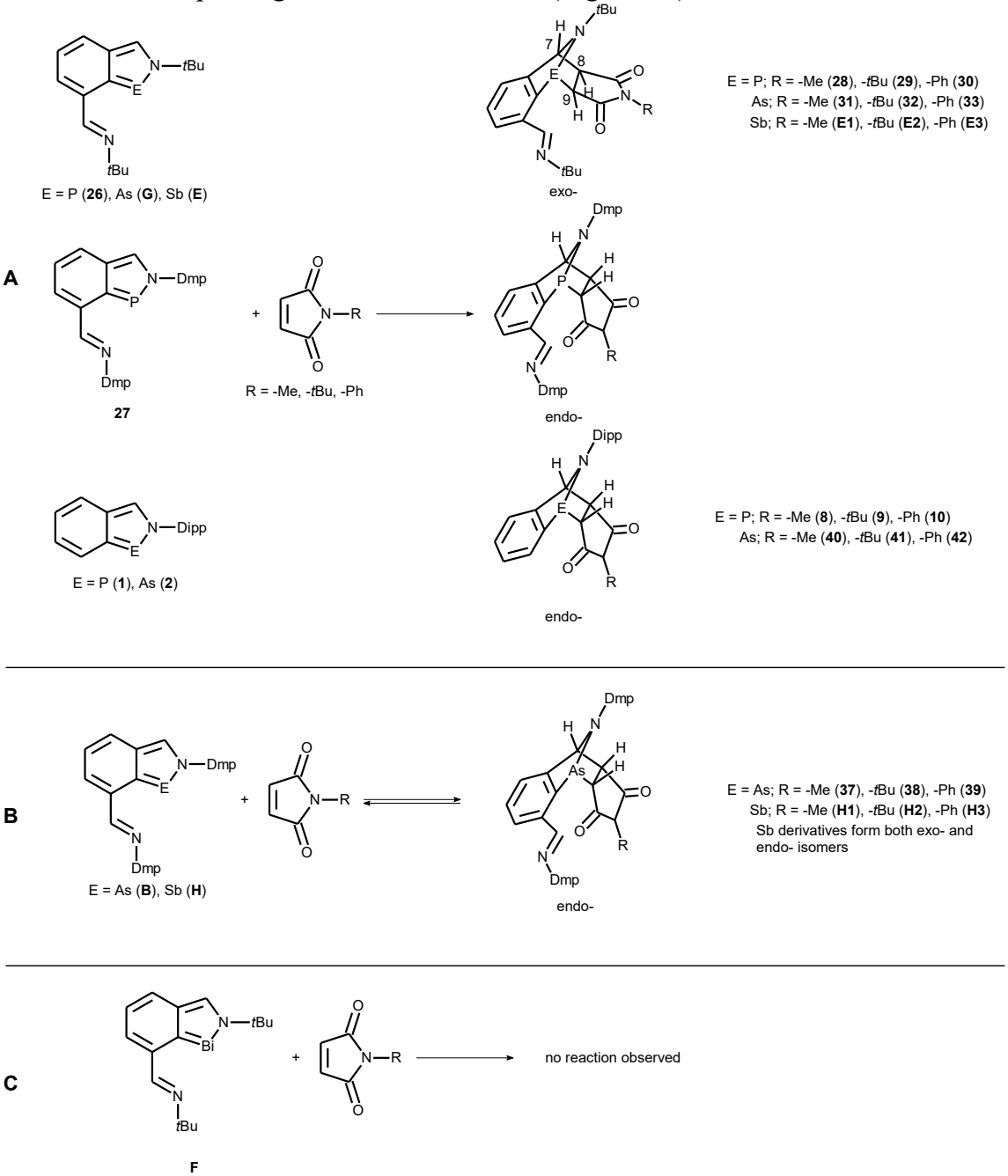

*Figure 28. Reaction of **26**, **G**, **E**, **F**, **27**, **B**, **H**, **1** and **2** with* N-*substituted maleimides*

All newly prepared and isolated compounds were characterized by NMR analysis. The most notable similarity all the prepared compounds share, is the presence of an ABX spin system involving the *H*7, *H*8 and *H*9 hydrogen atoms. The value of the ^{3}J(*H*7, *H*8) coupling constant allows the differentiation between exo- (J = 0.7 – 1.6 Hz) and endo- (J = 5.5 – 5.7 Hz) isomers, thus providing a useful way to determine the

stereoisomer even in solution. Interestingly, the isolated compounds highly prefer only one of the two isomers.

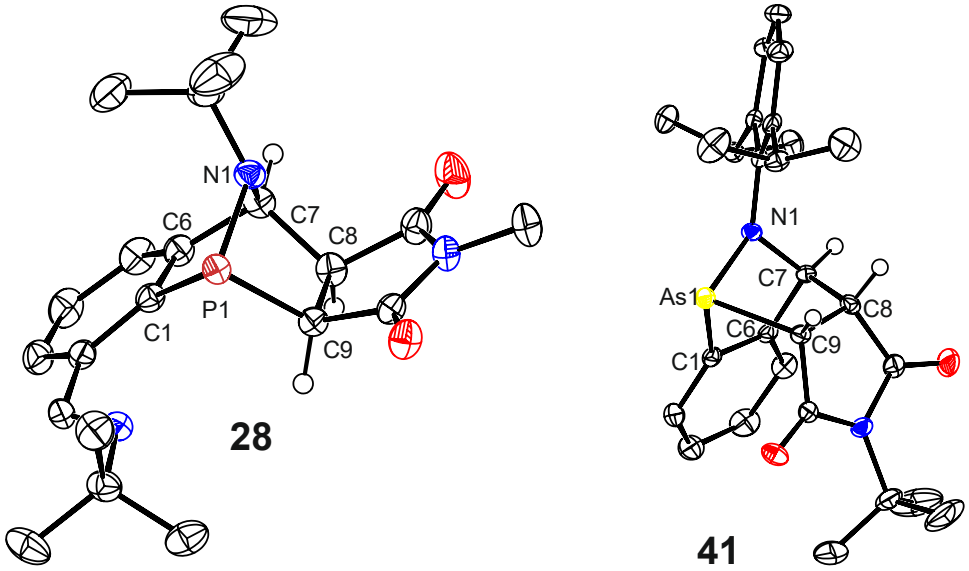

*Figure 29. Comparison of the exo- (**28**) and the endo- (**41**) isomers*

An exceptional behaviour was observed in the case of the starting compounds **B** and **H**. In their cases, the cycloadducts were not isolated because of the prevalent reverse reaction, which did not allow for the crystalisation of the final products **37** – **39** and **H1** – **H3** (Figure 28B). Nevertheless, it was possible to prepare the reaction mixtures in toluene-d_8, which was used further (*vide infra*). Moreover, for the bismuth starting compound **F** no reaction with any of the maleimides was observed (Figure 28C) even when cooled to 223 K.

The prepared cycloadducts or the reaction mixtures of **37** – **39** and **H1** – **H3** were studied via variable temperature ^{1}H NMR spectroscopy in toluene-d_8 in order assess the thermodynamic parameters (ΔG° and ΔH°) of these cycloaddition reactions.

According to the acquired values of ΔG°, the reverse reaction is the more prevalent the heavier central atom is used. On the other hand, no clear trend can be drawn from changing the maleimide substituent. This is not the case when looking at the two different N,C,N chelating ligands. The -*t*Bu substituted N,C,N (N,C,N$^{t\text{Bu}}$) directs the cycloaddition clearly toward the exo- product, while the -Dmp substituted ligand (N,C,N$^{\text{Dmp}}$) prefers the formation of the endo- isomers. At the same time, the negative ΔG° values for N,C,N$^{\text{Dmp}}$ are closer to 0 compared to N,C,N$^{t\text{Bu}}$, which indicates the equilibrium shift toward the starting compounds in the case of N,C,N$^{\text{Dmp}}$ ligand.

When considering the -Dipp substituted C,N chelating ligand (C,N$^{\text{Dipp}}$), it is notable, that only endo- isomers are formed. It indicates, that the pendant imino group does not influence the stereoselectivity of the reaction, rather it is affected by the steric bulk of the imino substituent involved in the reaction. Furthermore, the thermodynamic data show similar or even more negative values than the compounds chelated by the N,C,N$^{t\text{Bu}}$ ligand, which points to the fact, that the pendant imino group might be destabilising the final product and thus making the compounds containing C,N$^{\text{Dipp}}$ ligand generally more stable.

To summarise, several starting compounds **26**, **G**[5], **E**[9], **F**[10], **27**, **B**[2], **H**[11], **1** and **2** containing different pnictogen atoms and ligands (N,C,N$^{t\text{Bu}}$, N,C,N$^{\text{Dmp}}$ a C,N$^{\text{Dipp}}$) reacted with *N*-substituted maleimides to give [4+2] cycloadducts as two possible isomers. The

N,C,N$^{t\text{Bu}}$ compounds afforded exo- isomers, while N,C,N$^{\text{Dmp}}$ a C,N$^{\text{Dipp}}$ prefer the formation of the endo- isomer. The reversibility of these reactions was studied through ΔG° and ΔH° data, which showed that heavier central atoms shift the reaction toward the starting compounds and the pendant imino group does not influence the preferred isomer, which appears to be mostly dependent on the stericity of the imino-group substituent involved in the reaction. Moreover, the presence of the pendant imino function in general lowers the stability of the adduct, thus shifting the reaction toward the starting compounds.

2.5 Synthesis and Reactivity of a 2,1-benzazaarsole Stabilized by a Non-symmetric N,C,N ligand

Based on previous findings made by our group[11], an N,C,N chelated aryldichlorostibine substituted by Dipp- groups reduced by potassium tri-*sec*-butylborohydride (K-Selectride) afforded a compound where not only the antimony atom was reduced, but also one of the pendant imino functions was saturated to form an amino group. Thus, a stibinidene stabilized by a non-symmetric N,C,N ligand was prepared.

Similar approach was applied on the starting compound **15**[a], which was used to gain **15** using KC_8 as a reducing agent. Using K-Selectride at -80 °C as a reductant afforded smoothly single crystals of **43** (Figure 30), which were analyzed using X-ray crystallography (Figure 31). Significant are the different distances between C7-N1 (1.339(6) Å) and C8-N2 (1.460(6) Å), corresponding to the double and single bond length respectively.

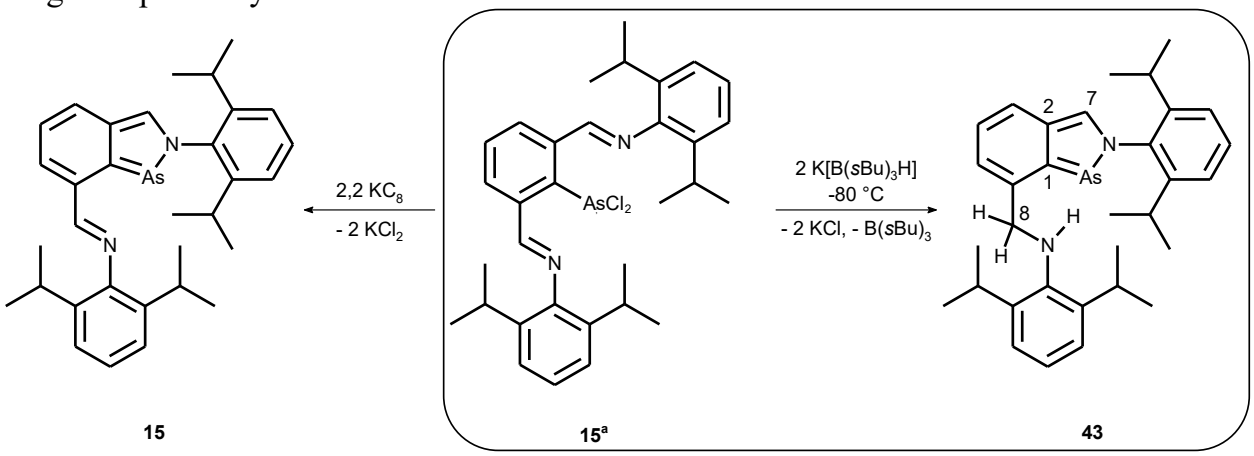

*Figure 30. Preparation of **43***

Compound **43** was also characterized by ^{1}H and $^{13}C\{^{1}H\}$ NMR spectroscopy, which shows a signal for the imino group *H*7 ($\delta(^{1}H)$ = 8.19 ppm), for *H*8 ($\delta(^{1}H)$ = 4.53 ppm) belonging to the newly formed amino group as well as the corresponding N*H* signal ($\delta(^{1}H)$ = 3.96 ppm).

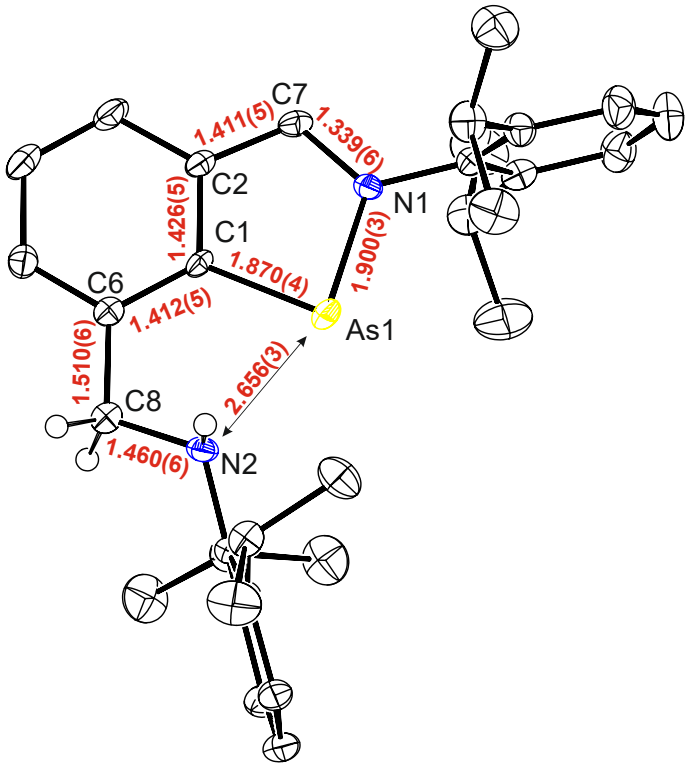

*Figure 31. Molecular structure of **43** including selected distances*

To assess the influence of the steric bulk of the imino group substituents, three additional dichloroarylarsines **B**[a], **G**[a] and **44**[a] were isolated. While **B**[a] and **G**[a] were already used *in-situ* to produce the formally monovalent **B**[2] and **G**[5], this is the first time they were isolated and characterized in order to limit the side reactions of possible impurities with K-Selectride. All three compounds were prepared by lithiation of the arylbromide and subsequent treatment by $AsCl_3$ and isolated as crystalline solids. **B**[a] was additionally characterised using X-ray crystallography, showing different distances between As1-N1 (2.197(5) Å) and As1-N2 (2.361(5) Å). The ^{1}H and $^{13}C\{^{1}H\}$ NMR spectra show *H*5 ($\delta(^{1}H)$ =7.89 – 8.72 ppm) and *C*5 (δ ($^{13}C\{^{1}H\}$ = 158.2 – 166.4 ppm).

All three precursors were subsequently reduced using K-Selectride at – 80 °C. In the case of **G**[a] and **44**[a], a mixture of products was isolated, while **B**[a] afforded a pure product **45**. The compound **44**[a] was also reduced by KC_8, which gave after workup the formal arsinidene **44** (Figure 32).

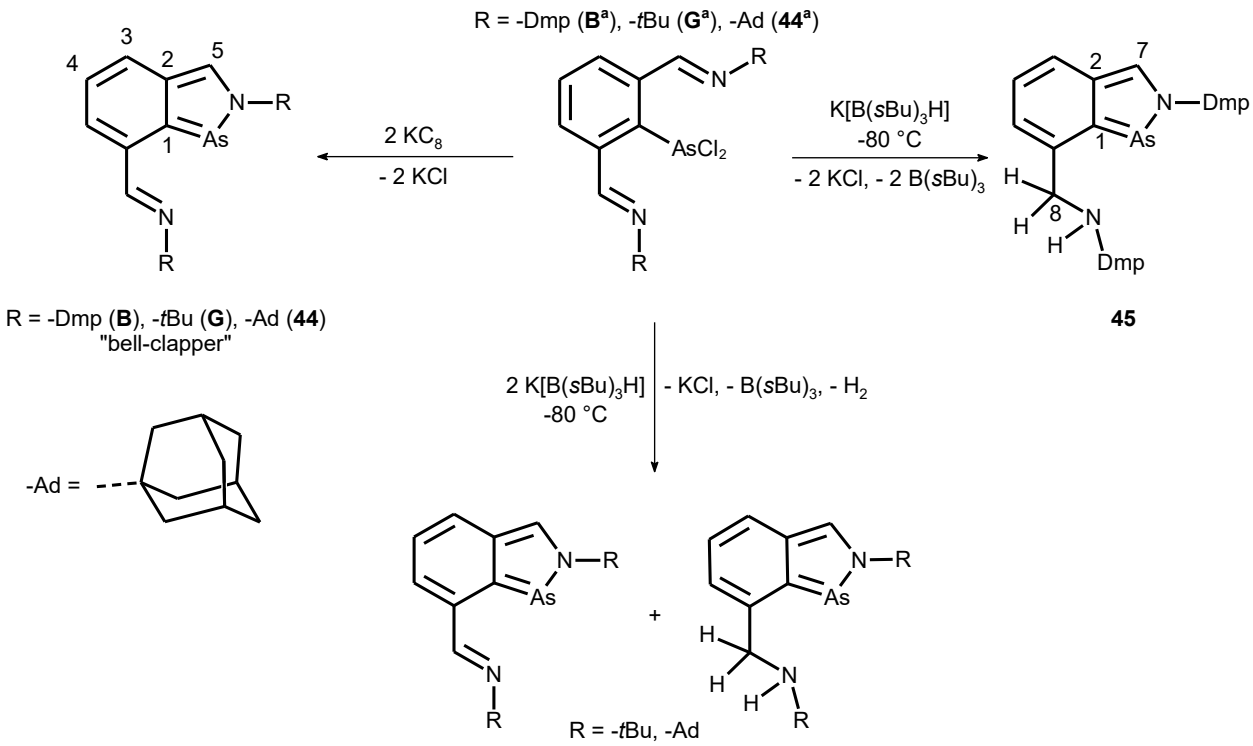

Figure 32. The influence of differently substituted N,C,N ligands on the product of the reduction using K-Selectride

The NMR spectra of **44** show *H*5 ($\delta(^1H)$ = 8.64 ppm) and *C*5 ($\delta(^{13}C\{^1H\})$ = 146.1 ppm) signals. The mixtures of products obtained after reducing **G[a]** and **44[a]** using K-Selectride show the presence of two sets of signals in ^1H NMR spectra. Apart from the arsinidenes **44** and **G**[5], the presence of the target non-symmetric product was confirmed by the observable *H*7 ($\delta(^1H)$ = 8.44; 8.56 ppm), *H*8 ($\delta(^1H)$ = 3.92; 4.01 ppm) and N*H* groups ($\delta(^1H)$ = 1,14; 1.18 ppm).

^1H and $^{13}C\{^1H\}$ NMR spectra of the compound **45** show signals for *H*7 ($\delta(^1H)$ = 7.73 ppm), *H*8 ($\delta(^1H)$ = 4.31 ppm) and N*H* ($\delta(^1H)$ = 3.55 ppm), as well as the corresponding carbon signals of *C*7 ($\delta(^{13}C\{^1H\}$ = 140.9 ppm) and *C*8 ($\delta(^{13}C\{^1H\}$ = 54.5 ppm).

A noticeable trend is evident based on these K-Selectride reduction products. The starting compounds **15[a]** and **B[a]** containing aromatic substituents, afforded pure hydrogenation products **43** and **45**. On the other hand, starting compounds **44[a]** and **G[a]** containing aliphatic substituents led to mixtures of products.

Moreover, the compound **43** was studied as to describe its reactivity toward dienophiles. First, **43** was treated with DMAD to give the cycloadduct **46** (Figure 33).The NMR spectra show a signal for *H*7 ($\delta(^1H)$ = 6.22 ppm) and *C*7 ($\delta(^{13}C\{^1H\})$ = 83.7 ppm). They also display two signals for the *H*10 methylene group hydrogen atoms ($\delta(^1H)$ = 3.91; 4.45 ppm). Infrared and Raman spectra show the amino group at 3350 cm^{-1} and carbonyl groups at 1710 cm^{-1}.

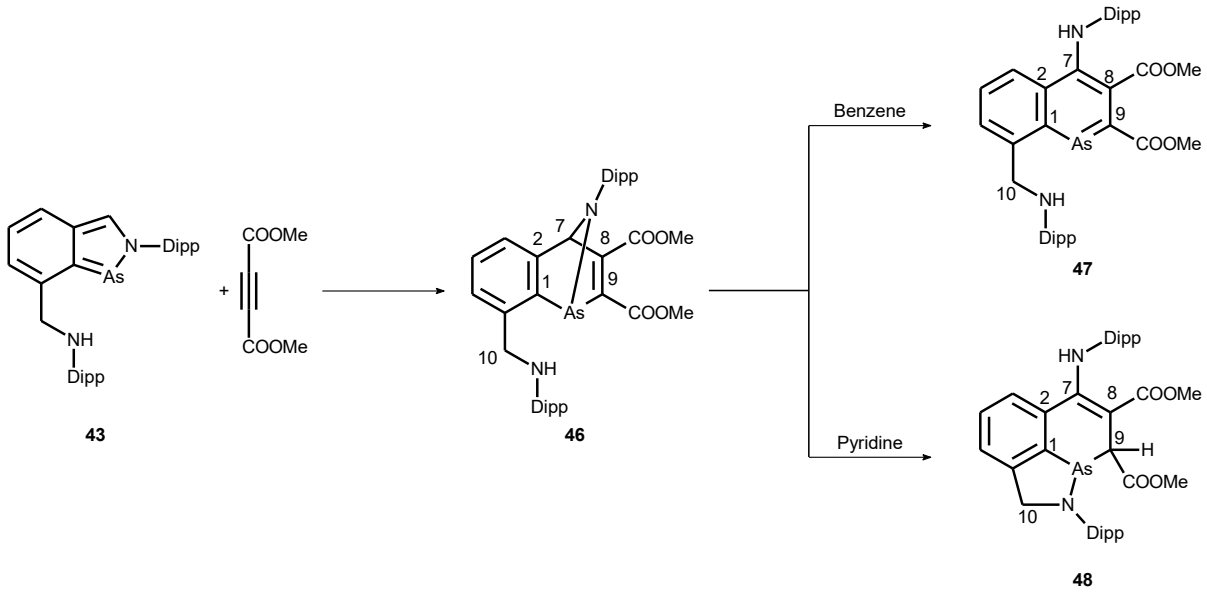

*Figure 33. Preparation of **46** – **48***

Next, the compound **46** was heated in benzene to give the product **47** (Figure 33). X-ray structure shows the molecular structure of a 1-arsanaphthalene derivative with relevant C-C bond lengths between 1.367(3) and 1.451(2) Å.

The NMR spectra depict the newly formed N*H* group ($\delta(^1H)$ = 9.13 ppm) and a single signal belonging to the *H*10 hydrogen atoms ($\delta(^1H)$ = 4.73 ppm).

As per the strategy already discussed, pyridine was used as a proton transfer agent. **46** was therefore also heated in pyridine, however the reaction did not yield 1-arsanaphthalene derivative. Rather, a new product **48** was formed (Figure 33). The product was characterized using X-ray crystallography (Figure 34), which shows that the pendant amino group formed an As1-N2 bond (1.849(2) Å) toward the As central atom. Further, **48** was analysed by NMR spectroscopy, which revealed a new *H*9 signal ($\delta(^1H)$ = 4.91 ppm) and differentiated *H*10 hydrogens ($\delta(^1H)$ = 4,68; 5,02 ppm). The vibrational spectra show a band assigned to the C=O bond at 1717 cm^{-1}.

This reaction was also monitored using ^1H NMR spectroscopy, revealing **47** as an intermediate. The pendant amino group therefore significantly influences the reactivity of **46**. In fact, the formation of the compound **48** is dependent on the amino group's presence.

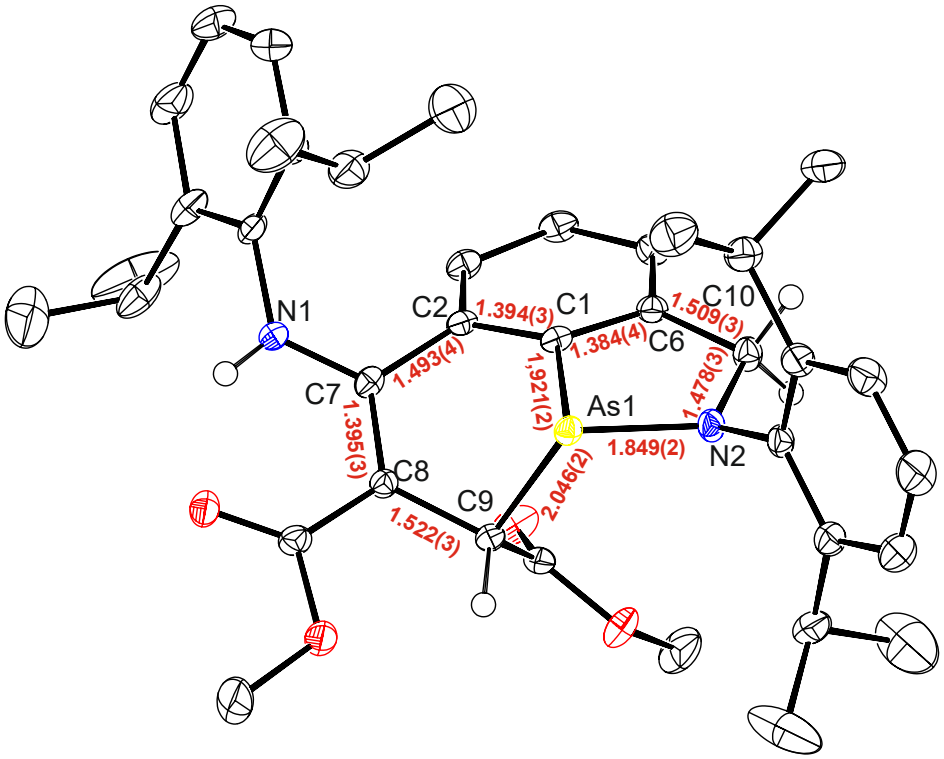

*Figure 34. Molecular structure of **43** including selected distances*

Finally, being inspired by the use of a bismuthinidene as a catalyst[6,7], the starting compound **43** was treated with atmospheric oxygen to give the product of oxidation **49** (Figure 35). Similar procedure applied to N,C,N chelated pnictinidenes containing two imino groups produces only a complicated mixture of products. ^{1}H NMR spectra of **49** show a signal of the newly formed O*H* group ($\delta(^{1}H)$ = 1.94 ppm) and the two diastereotopic hydrogens *H*8 ($\delta(^{1}H)$ = 4.40; 5.10 ppm). In the IR and Raman spectra a band assigned to the OH group is visible (3602 cm^{-1}).

The following attempt to regenerate the starting **43** using pinacolborane[7] was only partly successful. Even though **43** was obtained (Figure 35), the reaction time was too long to justify any further research into possible catalytic functionality.

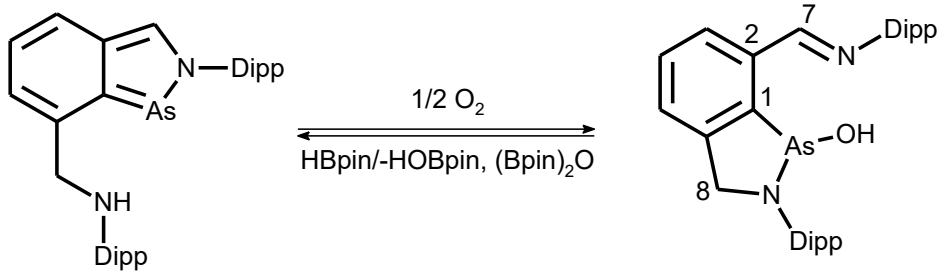

43 **49**

*Figure 35. The oxidation and regeneration of **43***

To summarise, the reactivity of **43** toward dienophiles was successfully studied. Due to the presence of a pendant amino group, the formed cycloadducts exhibit interesting new reactivity, most noticeably due to the formation of **48**. Furthermore, oxidation of **43** afforded **49**.

3 Closing Remarks

In coclusion, the ability of C,N and N,C,N chelated phosphinidenes and arsinidenes to act as hidden heterodienes was demonstrated on their tendency to take part in hetero-Diels-Alder reactions. Moreover, the reversibility of several of these cycloaddition reactions shows the potential of these substrates as candidates for catalytic use. Last but not least, an arsinidene coordinated by a non-symmetric N,C,N chelating ligand containing an imino and an amino function was prepared. Unique properties of this compound allowed for the successful reaction with oxygen and subsequent regeneration of the starting compound. Based on these findings it can be concluded that the reactivity of the discussed heteropnictoles presents additional research field, especially considering the possible application in catalysis.

4 References

1 J. Hyvl, W. Y. Yoshida, A. L. Rheingold, R. P. Hughes and M. F. Cain, *Chem. Eur. J.*, 2016, **22**, 17562–17565.

2 V. Kremláček, *C,N-chelated Organoarsenic(I) Compounds – Synthesis, Structure and Coordination of Transition Metals*,Univerzita Pardubice, 2017.

3 P. Šimon, F. De Proft, R. Jambor, A. Růžička and L. Dostál, *Angew. Chem., Int. Ed.*, 2010, **49**, 5468–5471.

4 L. Liu, D. A. Ruiz, D. Munz and G. Bertrand, *Chem*, 2016, **1**, 147–153.

5 I. Vránová, V. Kremláček, M. Erben, J. Turek, R. Jambor, A. Růžička, M. Alonso and L. Dostál, *Dalton Trans.*, 2017, **46**, 3556–3568.

6 F. Wang, O. Planas and J. Cornella, *J. Am. Chem. Soc.*, 2019, **141**, 4235–4240.

7 Y. Pang, M. Leutzsch, N. Nöthling and J. Cornella, *J. Am. Chem. Soc.*, 2020, **142**, 19473–19479.

8 N. Tokitoh, T. Matsumoto and T. Sasamori, *Heterocycles*, 2008, **76**, 981–987.

9 M. Kořenková, M. Hejda, M. Erben, R. Jirásko, R. Jambor, A. Růžička, E. Rychagova, S. Ketkov and L. Dostál, *Chemistry*, 2019, **25**, 12884–12888.

10 I. Vránová, M. Alonso, R. Lo, R. Sedlák, R. Jambor, A. Růžička, F. De Proft, P. Hobza and L. Dostál, *Chem. Eur. J.*, 2015, **21**, 16917–16928.

11 I. Vránová, M. Alonso, R. Jambor, A. Růžička, J. Turek and L. Dostál, *Chem. Eur. J.*, 2017, **23**, 2340–2349.

5 List of Articles Published by The Author

Articles discussed in the doctoral thesis:

1. *Heterocycles Derived from Generating Monovalent Pnictogens within NCN Pincers and Bidentate NC Chelates: Hypervalency versus Bell-Clappers versus Static Aromatics.* V. Kremláček, J. Hyvl, W. Y. Yoshida, A. Růžička, A. L. Rheingold, J. Turek, R. P. Hughes, L. Dostál and M. F. Cain. *Organometallics* 2018, **37**, 2481–2490. **DOI: 10.1021/acs.organomet.8b00290**

2. *Non-conventional Behavior of a 2,1-benzazaphosphole: Heterodiene or Hidden Phosphinidene?.* V. Kremláček, E. Kertész, Z. Benkö, M. Erben, R. Jirásko, A. Růžička, R. Jambor and L. Dostál. *Chem. Eur. J.* **DOI: 10.1002/chem.202101686**

3. *From a 2,1-Benzazaarsole to Elusive 1-Arsanaphthalenes in One Step.* V. Kremláček, M. Erben, R. Jambor, A. Růžička, J. Turek, E. Rychagova, S. Ketkov and L. Dostál. *Chem. Eur. J.* 2019, **25**, 5668–5671. **DOI: 10.1002/chem.201900805**

4. *Hetero Diels–Alder Reactions of Masked Dienes Containing Heavy Group 15 Elements.* M. Kořenková, V. Kremláček, M. Hejda, J. Turek, R. Khudaverdyan, M. Erben, R. Jambor, A. Růžička and L. Dostál. *Chem. Eur. J.* 2020, **26**, 1144–1154. **DOI: 10.1002/chem.201904953**

5. *Probing the limits of a C=C bond activation by N-coordinated organopnictogen(I) compounds.* V. Kremláček, M. Hejda, E. Rychigova, S. Ketkov, R. Jambor, A. Růžička and L. Dostál. *Eur. J. Inorg. Chem.* **DOI: 10.1002/ejic.202100648**

Articles outside of the scope of the doctoral thesis:

6. *A comparative study of the structure and bonding in heavier pnictinidene complexes [(ArE)M(CO)n] (E = As, Sb and Bi; M = Cr, Mo, Wand Fe)*. I. Vránová, V. Kremláček, M. Erben, J. Turek, R. Jambor, A. Růžička, M. Alonso and L. Dostál. *Dalton Trans*. 2017, **46**, 3556–3568. **DOI: 10.1039/c7dt00095b**

7. *Reactions of N,C,N-chelated pnictinidenes with Rh(I) and Ir(I) complexes: Coordination vs. Transmetalation.* M. Kořenková, V. Kremláček, M. Erben, R. Jambor, Z. Růžičková and L. Dostál. *J. Organomet. Chem*. 2017, **845**, 49–54. **DOI: 10.1016/j.jorganchem.2017.02.022**

8. *Heavier pnictinidene gold(i) complexes.* M. Kořenková, V. Kremláček, M. Erben, R. Jirásko, F. De Proft, J. Turek, R. Jambor, A. Růžička, I. Císařová and L. Dostál. *Dalton Trans.* 2018, **47**, 14503–14514. **DOI: 10.1039/C8DT03022G**